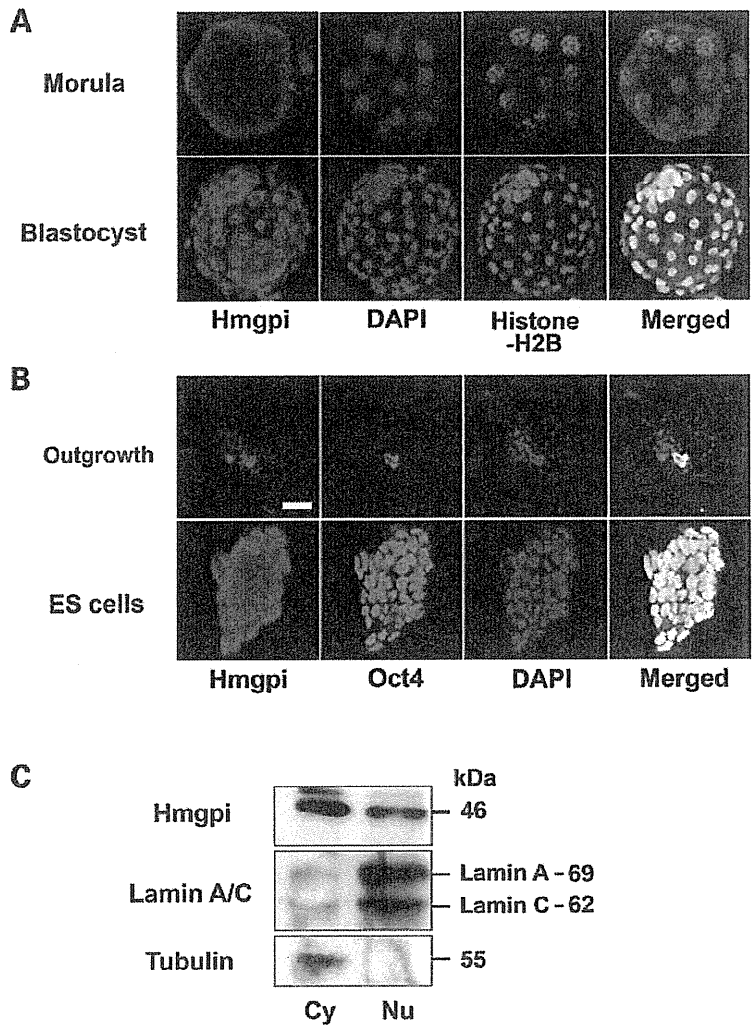

Figure 3. Localization of HMGPI in preimplantation embryos. (**A**) Nuclear translocation of HMGPI protein at the blastocyst stage. HMGPI was mainly detected in the cytoplasm of preimplantation embryos (from 4-cell embryos to morulae), but in the nuclei of blastocysts. Nuclei are shown by immunostaining with an anti-Histone-H2B antibody (green) and DAPI staining (blue). (**B**) Confocal microscopy images of blastocyst outgrowth and ES cells stained with antibodies to *Hmgpi* and *Oct4*, and with DAPI. Scale bar = 50 μM. (**C**) Western blotting analysis of HMGPI in cytoplasmic (Cy) and nuclear (Nu) fractions of ES cells. Lamin A/C and tubulin were used as markers of the nuclear and cytoplasmic fractions, respectively.

We then performed qRT–PCR analysis using α-amanitin to investigate *de novo* (zygotic) transcription of the *Hmgpi* gene. The supplementation of α-amanitin during *in vitro* culture from the 1-cell stage significantly reduced *Hmgpi* mRNA expression in the 2-cell embryos at post-hCG 43 and 53 h (early and late 2-cell stage, respectively) (Fig. 2D), implying that *Hmgpi* is transcribed zygotically during the major burst of ZGA, but not maternally.

To study the temporal and spatial expression pattern of the *Hmgpi*-encoded protein (HMGPI), we raised a polyclonal antibody against *Hmgpi* peptides. Western blot analysis of extracts from the mouse blastocysts showed only a single band corresponding to 46 kDa detected by the anti-HMGPI antibody. In addition, preincubation with the HMGPI peptide antigen abolished detection of the HMGPI protein, while preincubation with a control peptide had no effect on the immunodetection (Supplementary Material, Fig. S1). Although *Hmgpi* transcription started at the 2-cell stage, peaked at the 4-cell stage and then gradually decreased until the blastocyst stage (Fig. 2C), immunostaining and immunoblotting analysis revealed HMGPI expression from the 4-cell stage until the blastocyst stage, indicating a delayed expression pattern of HMGPI compared with that of the *Hmgpi* transcript. It was also notable that both ICM cells and trophectodermal cells retained HMGPI expression in blastocysts.

On the other hand, immunostaining for HMGPI in preimplantation embryos showed a unique subcellular localization pattern. Although a putative nuclear protein due to its role

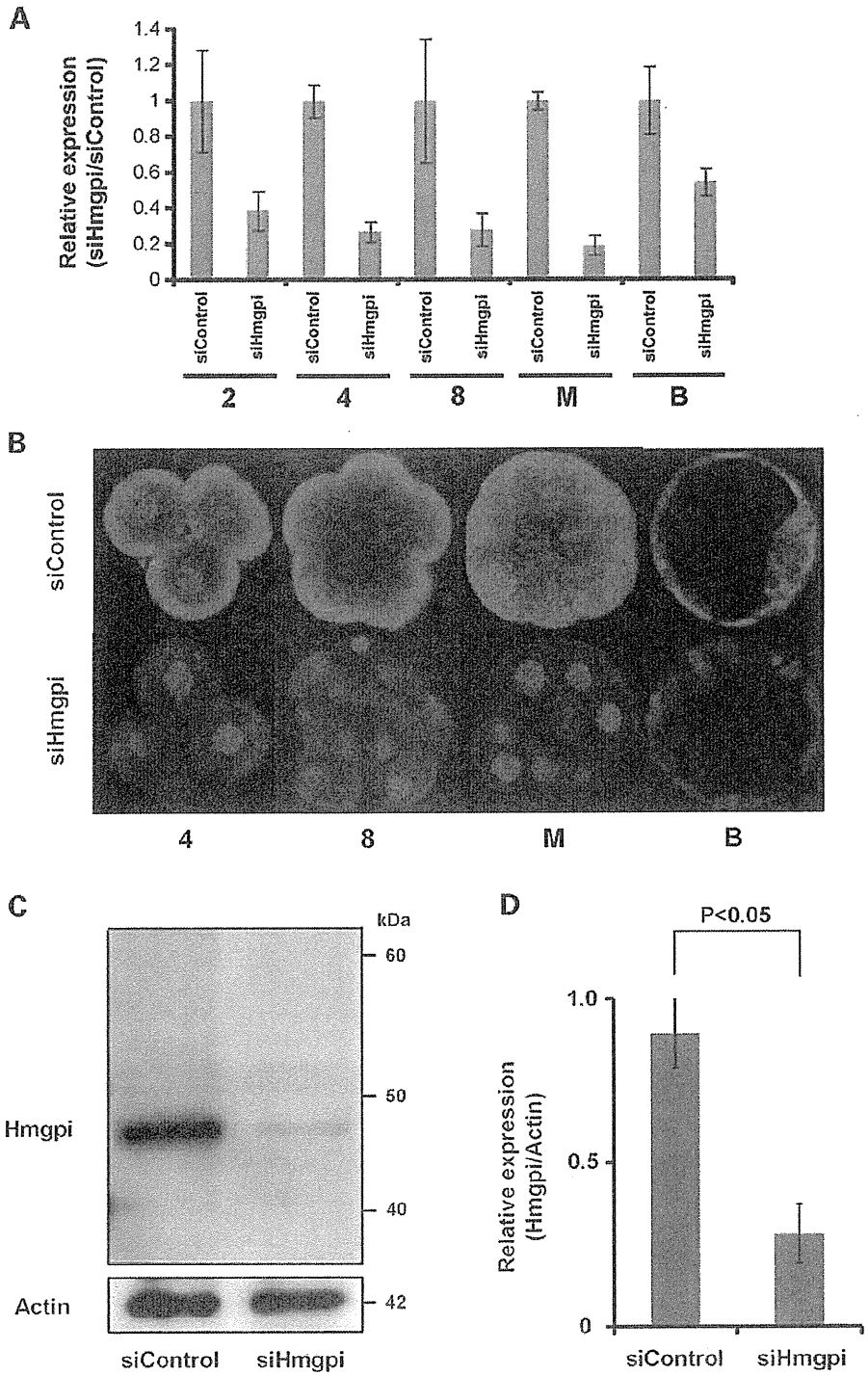

Figure 4. Loss-of-function study by siRNA technology. (A) Transcript levels of *Hmgpi* in embryos injected with control siRNA (siControl) and *Hmgpi* siRNA (siHmgpi) by real-time quantitative RT–PCR analysis. The expression levels were normalized using *H2afz* as a reference gene. Values are means ± SE for four separate experiments. (B) Laser scanning confocal microscopy images of HMGPI protein expression in a 4-cell embryo, 8-cell embryo, morula and blastocyst after injection with siControl or siHmgpi (red, HMGPI; blue, chromatin). (C and D) Immunoblot analysis of HMGPI expression at the blastocyst stage in siControl-injected and siHmgpi-injected embryos. The relative amount of HMGPI (46 kDa) was determined at the blastocyst stage (left: siControl-injected embryos, right: siHmgpi-injected embryos). The expression levels were normalized using actin expression (42 kDa) as a reference. Values are means ± SE from three separate experiments.

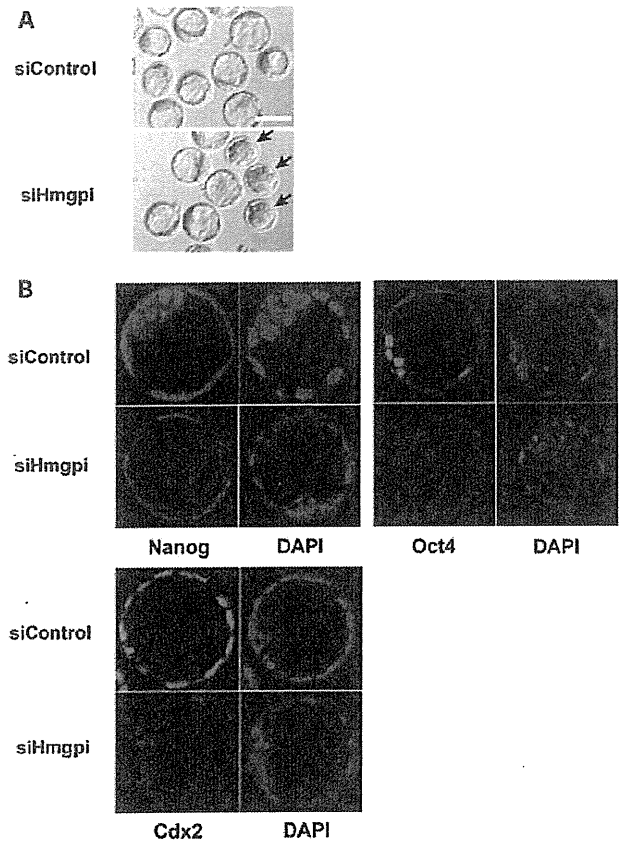

Figure 5. Function of *Hmgpi* in preimplantation development. (**A**) A pair of representative photos showing the development of embryos injected with *Hmgpi* siRNA (siHmgpi) and Control siRNA (siControl). The siHmgpi-injected embryos arrested at the morula stage are indicated by arrows. Scale bar = 100 μM. (**B**) For Nanog, Oct4 and Cdx2 immunostaining, all blastocysts in the siHmgpi-injected and siControl-injected groups were processed simultaneously. The laser power was adjusted so that the signal intensity was below saturation for the developmental stage that displayed the highest intensity and all subsequent images were scanned at that laser power. This allowed us to compare signal intensities for Nanog, Oct4 and Cdx2 expression between the siHmgpi-injected and siControl-injected embryos (Supplementary Material, Table S2).

as a transcription factor, HMGPI was detected mainly in the cytoplasm without any evidence of a nuclear localization from the 4-cell to the morula stage, suggesting a role other than transcriptional regulation (Fig. 2E). In contrast, HMGPI was localized to the nuclei rather than to the cytoplasm of blastocysts (Figs 2E and 3A). During blastocyst outgrowth, HMGPI was expressed in the nuclear region of most outgrowing cells, with scant amounts detected in the cytoplasm (Fig. 3B). Interestingly, Oct4-positive cells derived from the ICM showed particularly strong positive staining for HMGPI in the nucleus, suggesting a specific role as a nuclear protein in ES cells (Fig. 3B). On more closely examining HMGPI in ES cells, we found that almost all the Oct4-positive undifferentiated ES cells in a colony also expressed HMGPI (Fig. 3B), and immunoblotting confirmed HMGPI expression in both nuclear and cytoplasmic fractions of ES cells (Fig. 3C).

Effect of siRNA on *Hmgpi* mRNA level and protein synthesis

To investigate a role of *Hmgpi* in early embryonic development, we knocked down *Hmgpi* expression in mouse preimplantation embryos. We employed an oligonucleotide-based siRNA (denoted here siHmgpi and obtained from PE Applied Biosystems, Foster City, CA, USA). Zygotes injected with *Hmgpi* siRNAs (siHmgpi) or control siRNA (siControl) and non-injected zygotes as negative controls were cultured. *Hmgpi* expression was severely suppressed in the siHmgpi-injected embryos, and significantly lower than those in the siControl-injected or non-injected embryos (Fig. 4A). The siControl-injected embryos did not show any difference from the non-injected embryos in *Hmgpi* expression (data not shown). In addition, immunofluorescent staining clearly demonstrated that the siRNA injection reduced HMGPI protein expression in an individual preimplantation embryo (Fig. 4B). In the same set of experiments, the HMGPI levels were also assayed by western blotting (Figs 4C and 4D). HMGPI expression was significantly reduced in siHmgpi-injected blastocysts (0.89 ± 0.10) compared with that in negative controls (0.28 ± 0.08; $P < 0.05$).

Furthermore, we confirmed that siHmgpi had no influence on the expression of other genes with sequence similarities to *Hmgpi*, namely *Ubtf*, *Hmgb1*, *Hmgb2* and *Hmgb3*. Although *Ubtf*, *Hmgb1*, *Hmgb2* and *Hmgb3* were all expressed in control preimplantation embryos, the siHmgpi construct used in this study did not affect the expression of these genes in the siHmgpi-injected embryos (Supplementary Material, Fig. S2). On the other hand, it has been demonstrated that loss-of-function of these genes produces no distinct phenotypes at the pre- and peri-implantation stages (21).

Effect of *Hmgpi* siRNA on preimplantation development

To study the function of *Hmgpi* during preimplantation development, siHmgpi-injected or siControl-injected zygotes were cultured *in vitro* until the blastocyst stage. The embryos injected with siHmgpi at 21–23 h after hCG administration often failed to become blastocysts at 3.5 days postcoitum (dpc) (Fig. 5A). In addition, the reduction in Hmgpi expression significantly suppressed preimplantation development, whereby $68.9 \pm 1.3\%$ of siHmgpi-injected embryos became blastocysts, while $94.1 \pm 1.3\%$ of siControl-injected embryos reached the blastocyst stage (Supplementary Material, Fig. S3; $P < 0.0001$). Most of the siHmgpi-injected embryos that failed to become blastocysts showed developmental arrest after the morula stage and did not appear to form blastocoels, suggesting impairment of trophectodermal development (Supplementary Material, Fig. S3). To analyze the phenotype of siHmgpi-injected embryos further, we performed immunofluorescence staining of lineage-specific markers such as Cdx2, Nanog and Oct4 at the blastocyst stage. Although siHmgpi-injected embryos that reached the blastocyst stage appeared morphologically intact, the expression of lineage-specific markers was reduced (Fig. 5B). Cdx2, which is required for implantation and extra-embryonic development, was particularly and markedly down-regulated in trophectodermal cells, while Nanog and Oct4

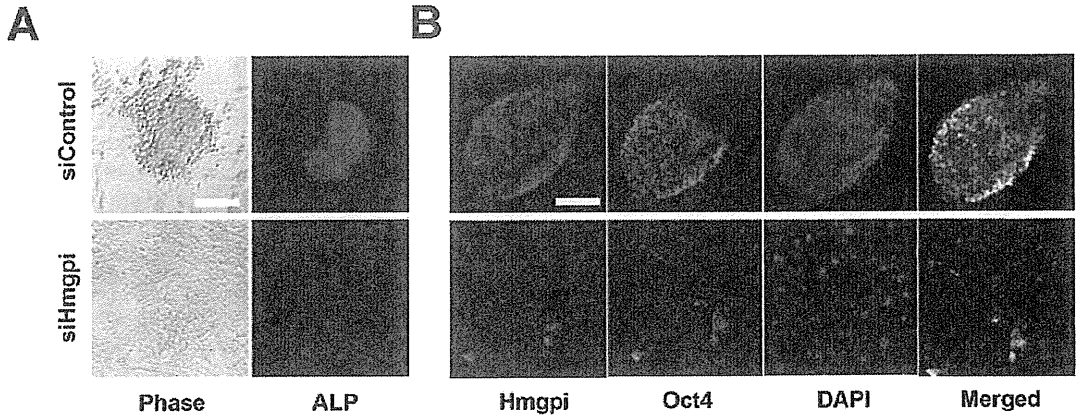

C

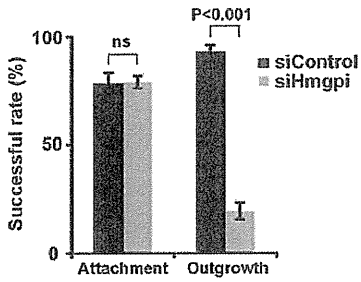

	Tested blastocysts	Attachment (%)	Outgrowth (%)
siControl	51	34 (66.6)	30 (88.2)
siHmgpi	20	15 (75.0)	2 (13.3)
siControl	117	92 (78.6)	80 (86.9)
siHmgpi	13	10 (76.9)	2 (20.0)
siControl	55	49 (89.0)	48 (97.9)
siHmgpi	8	7 (87.5)	1 (14.2)
siControl	41	33 (80.4)	33 (100.0)
siHmgpi	13	10 (76.9)	3 (30.0)

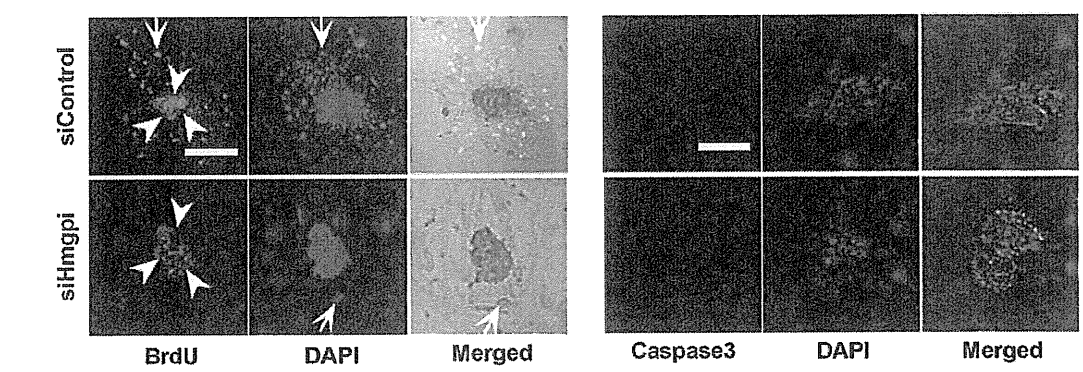

F

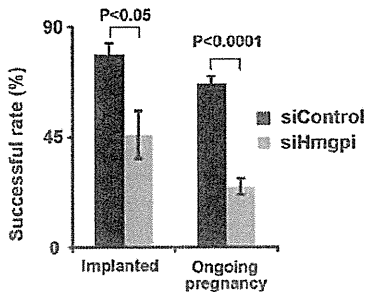

	Transferred embryos	Implanted (%)	Ongoing pregnancy (%)
siControl	30	23 (76.7)	20 (66.7)
siHmgpi	18	6 (33.3)	3 (16.7)
siControl	30	25 (83.3)	18 (60.0)
siHmgpi	32	20 (62.5)	10 (31.2)
siControl	16	13 (81.2)	12 (75.0)
siHmgpi	24	15 (62.5)	7 (29.1)
siControl	20	13 (65.0)	13 (65.0)
siHmgpi	32	8 (25.0)	7 (21.8)

were likewise downregulated in ICM cells of the siHmgpi-injected embryos (Fig. 5B and Supplementary Material, Table S2). Thus, *Hmgpi* is essential for the earliest embryonic development; both ICM and trophectodermal development.

Effect of *Hmgpi* siRNA on *in vivo* and *in vitro* peri-implantation development

To investigate the role of *Hmgpi* in proliferation of the ICM and trophectodermal cells, siHmgpi-injected and siControl-injected embryos were further cultured *in vitro* from the blastocyst stage, and attachment and outgrowth of each embryo on gelatin-coated culture plates was examined. HMGPI expression in siHmgpi-injected embryos was significantly reduced, and immunostaining showed that many colonies of ICM cells in the embryos collapsed during outgrowth culture (Fig. 6A and B). Although the vast majority of ICMs from siControl-injected embryos showed successful attachment (80.3 $\pm$ 4.9%) and vigorous outgrowth (96.2 $\pm$ 2.7%), those from siHmgpi-injected embryos failed to proliferate or produced only a residual mass (19.3 $\pm$ 3.8%) despite successfully attaching (79.0 $\pm$ 2.8%) (Fig. 6C; attachment ns; outgrowth, $P < 0.001$). These results implied that *Hmgpi* is essential for proliferation of ICM and trophectodermal cells in peri-implantation development, and for derivation of ES cells.

We then investigated cell proliferation and apoptosis during blastocyst outgrowth. Comparable incorporation of BrdU in blastocyst outgrowths of siHmgpi-injected embryos was less than that of siControl-injected embryos. Proliferation was significantly reduced in ICM-derived cells and dramatically suppressed in trophoblast cells (Fig. 6D). Embryonic fibroblasts were used as a feeder layer in this study and could support ICM cells, thus proliferation should have proceeded regardless of trophectodermal cell support. Therefore, the collapsed ICM-derived colonies in the current experiment were not a secondary effect of reduced proliferation in trophoblast cells, but a direct effect of the siHmgpi-induced decrease in ICM proliferation. Apoptosis was not detected in any cells during blastocyst outgrowth of siHmgpi-injected embryos, based on the absence of active caspase3 (Fig. 6E). Taken together, these findings show that *Hmgpi* is indispensable for proliferation of the ICM and trophectodermal cells in peri-implantation development and for the generation of ES cells.

Finally, we tested whether the experimental blastocysts could develop *in vivo* by transferring siHmgpi-injected and siControl-injected blastocysts into the uterus of pseudopregnant mice. Only 45.8 $\pm$ 9.7 and 24.7 $\pm$ 3.3% of blastocysts injected with siHmgpi implanted and developed, respectively, whereas most of the siControl-injected embryos showed successful implantation and ongoing development (76.5 $\pm$ 4.0 and 66.6 $\pm$ 3.3%, respectively) (Fig. 6F; implanted, $P < 0.05$; ongoing pregnancy, $P < 0.0001$). These results confirmed a role for *Hmgpi* in peri-implantation embryonic development.

DISCUSSION

We previously analyzed the dynamics of global gene expression changes during mouse preimplantation development (3). Understanding these preimplantation stages is important for both reproductive and stem cell biology. Many genes showing wave-like activation patterns (e.g. ZGA and MGA) during preimplantation were identified, and any or all of these may contribute to the complex gene regulatory networks. *Hmgpi*, one of the few novel preimplantation-specific genes, is involved in early development, implantation and ES cell derivation.

Structure-based prediction of *Hmgpi* function

Structural information about a protein sometimes hints at functional mechanisms, which remain unknown for *Hmgpi*'s clear role in early embryonic development. The HMG family proteins are abundant nuclear proteins that bind to DNA in a non-sequence-specific manner, influence chromatin structure and enhance the accessibility of binding sites to regulatory factors (17). Based on the number and the type of HMG domains, *Hmgpi* is relevant to the HMGB subfamily, characterized by containing two HMG-box domains ('HMG-box' or 'HMG-UBF_HMG-box'), rather than either the HMGA or HMGN subgroups. *Hmgpi* is also known as *Ubtfl1* in the NCBI gene database, based on sequence similarity to *Ubtf*, a well-known ZGA gene (3,22). *Ubtf*, encoding a SANT domain and six HMG-box domains, functions exclusively in RNA polymerase I (Pol I) transcription (23) and acts through its multiple HMG boxes to induce looping of DNA, which creates a nucleosome-like structure to modulate tran-

Figure 6. Function of *Hmgpi* in peri-implantation development. (**A**) Blastocyst outgrowth and alkaline phosphatase (AP) activity in the siHmgpi-injected and siControl-injected embryos, carried out according to a standard procedure (42). Representative images of phase-contrast microscopy for blastocyst outgrowth and fluorescent immunocytochemistry for AP are shown. Scale bar = 100 μM. (**B**) Confocal microscopy images of blastocyst outgrowth for the siHmgpi-injected and siControl-injected embryos, stained with antibodies to Hmgpi and Oct4. Nuclei are shown by DAPI staining. Scale bar = 100 μM. (**C**) Successful rate of blastocyst outgrowth for siHmgpi-injected and siControl-injected embryos. Successful outgrowth in this assay was indicated by the presence of proliferating cells after 6 days in culture. The experiment was repeated four times. (**D**) BrdU incorporation assay for blastocyst outgrowth of the siHmgpi-injected and siControl-injected embryos. Cell proliferation was determined by BrdU incorporation (ICM: arrowhead, trophectodermal cells: arrow). The trophectodermal component contained few cells and BrdU incorporation was confined to the ICM core; however, cell proliferation was reduced in the blastocyst outgrowth of siHmgpi-injected embryos compared with that of the siControl-injected embryos. Nuclei are shown by DAPI staining. Scale bar = 100 μM. (**E**) Immunocytochemistry with an anti-caspase3 antibody in blastocyst outgrowth of the siHmgpi-injected and siControl-injected embryos. Apoptotic cells were not apparent in the blastocyst outgrowth of either injected embryo. Nuclei are shown by DAPI staining. Scale bar = 100 μM. (**F**) Successful rate of siHmgpi-injected and siControl-injected embryo transfer. We transferred 3.5 dpc blastocysts into the uteri of 2.5 dpc pseudopregnant ICR female mice. The pregnant ICR mice were sacrificed on day 12.5 of gestation and the total numbers of implantation sites and of live and dead embryos/fetuses were counted. The experiment was repeated four times.

scription of the 45S precursor of ribosomal RNA (rRNA) by Pol I (24,25). Because the association of UBTF with rRNA genes *in vivo* is not restricted to the promoter and extends across the entire transcribed portion, UBTF promotes the formation of nucleolar organizer regions, indicative of 'open' chromatin (26). Based on the sequence similarity between UBTF and HMGPI, HMGPI might also bind to DNA in a non-specific manner, and modulate chromatin during peri-implantation when dynamic chromatin change is essential.

Alternatively, HMGPI may act as a cytokine during preimplantation development in a similar manner to HMGB1. HMGB proteins are found primarily in the cell nucleus, but also to varying extents in the cytosol (27,28), and have been suggested to shuttle between compartments (17). HMGB1 is indeed passively released from nuclei upon cell death and actively secreted as a cytokine (29), and the addition of recombinant HMGB1 into culture medium enhances *in vitro* development of mouse zygotes to the blastocyst stage in the absence of BSA supplementation (30). Although HMGPI failed to be detected in culture media after *in vitro* culture of preimplantation embryos or ES cells in this study (data not shown), two different modes of Hmgpi action, chromatin modulator and secreted mediator, should be taken into consideration as discussed later.

Role of *Hmgpi* during peri-implantation

The HMGPI protein was first detected in 4-cell embryos and then abundantly expressed in 8-cell embryos, morulae, ICM, trophectoderm and ES cells. Although *Hmgpi* transcription peaked at the 4-cell stage, the most dramatic siRNA effect appeared at the blastocyst and subsequent stages. This discrepancy between temporal expression and phenotype is attributed to three possible mechanisms. First, protein expression is generally delayed from transcription, indicated here by the *Hmgpi* transcripts and HMGPI protein expression peaking at the 4-cell stage and blastocyst stage, respectively. Similarly, *Stella* (31) and *Pms2* (32) are maternal-effect genes, but do not cause developmental loss until later preimplantation stages. A second possibility is the incompleteness of siRNA knockdown. One limitation of such knockdown experiments is the potential variability in levels of silencing of a target gene, which could in turn underlie the observed phenotypic variability in the present study. Embryos with complete suppression of Hmgpi may exhibit developmental arrest at earlier stages (e.g. at the morula stage), while those with less suppression may not display a phenotype until the later stages (e.g. at the implantation stage). Ideally, the suppression level of each embryo could be experimentally analyzed to correlate with the phenotype. The third possibility is spatial translocation of HMGPI protein in the blastocyst cells. The HMGPI expression pattern indicated differential spatial requirements during early embryogenesis, supported by the apparent ability of HMGPI to shuttle between the nucleus and the cytoplasm; the cytoplasmic HMGPI observed from the 4-cell to morula stages and the nuclear HMGPI in blastocysts and ES cells could have different functions. A bipartite nuclear localization signal (NLS) peptide (FKKEKEDFQKKMRQFKK) similar to NLS of HMGN2/HMG-17 (33) is also present in the HMGPI sequence. Thus, the nuclear HMGPI in blastocysts and ES cells might exert a critical transcriptional role to regulate gene expression essential for peri-implantation development. Indeed, the siHmgpi-induced knockdown of *Hmgpi* expression downregulated *Cdx2* in trophectodermal cells and *Oct4* and *Nanog* in ICM cells, with subsequently reduced proliferation of trophectodermal cells and ICM-derived cells during blastocyst outgrowth.

Genes indispensable for derivation of ES cells

Like *Hmgpi*, *Zscan4* is another exclusively zygotic gene not expressed at any other developmental stage (13). *Zscan4* is a putative transcription factor harboring a SCAN domain and zinc finger domains, and transcribed not only in preimplantation embryos but also in ES cells (13). Reduction of *Zscan4* by RNA interference showed a phenotype similar to that induced by *Hmgpi* knockdown: developmental deterioration at the preimplantation stages, especially cleavage pause at 2-cell stage, and failure in blastocyst outgrowth, ES-cell derivation and implantation. Thus, a preimplantation-specific gene expression pattern could indicate a function in ES-cell derivation and/or maintenance. Indeed, *Hmgpi* was also expressed in entire ES colonies, whereas *Zscan4* shows a peculiar mosaic expression pattern in undifferentiated ES cell colonies. Furthermore, the *Hmgpi* gene is highly expressed in ES cells, but not in EC cells; *Hmgpi* is thus eligible as a putative ECAT (ES cell-associated transcript), whose ESTs are overrepresented in cDNA libraries from ES cells compared with those from somatic tissues and other cell lines including EC cells (34). It is also likely that *Hmgpi* is expressed in iPS cells, based on *in silico* analyses of expression profiles [NCBI GEO database, e.g. GSE10806 (35)]. Thus, *Hmgpi* is likely to have a role in maintaining pluripotent cells, since the ECATs such as *Nanog*, *Eras* and *Gdf3* are required for pluripotency and proliferation of ES cells (34,36,37). In the current study, *Hmgpi* was indeed involved in blastocyst outgrowth of ICM cells. On the other hand, several genes including ECAT members have been implicated in trophectodermal development as well as in early embryonic development. Like *Hmgpi* that was expressed in both ICM cells and trophectodermal cells, *Dnmt3l/Ecat7* has a role in embryonic and extra-embryonic tissues in early developmental stages. *DNMT3L* is recruited by *DNMT3A2* to chromatin (38) to function in DNA methylation in ES cells, and defects in maternal *DNMT3L* induce a differentiation defect in the extra-embryonic tissue (39). The reduced CDX2 expression in blastocysts and poor BrdU incorporation during blastocyst outgrowth following siHmgpi knockdown suggested the potential involvement of *Hmgpi* in trophectodermal development.

In summary, *Hmgpi* is required early on in mammalian development to generate healthy blastocysts that implant successfully and produce ES cells. HMGPI translocates into the nucleus from cytoplasm at the blastocyst stage, which is importantly a turning point of early embryonic development when DNA-methylation levels are at their lowest and implantation takes place. The nuclear HMGPI in blastocysts and ES cells is expected to act as a transcription factor to regulate gene expression networks underlying the generation, self-renewal and maintenance of pluripotent cells. Because E7 embryos have already stopped expressing *Hmgpi*, it is likely

that *Hmgpi* stage-specifically regulates a set of genes that drive peri-implantation development. It will be valuable to identify both cofactors that bind HMGPI and recognize specific DNA sequences, as well as genes that are regulated by *Hmgpi* using ES cells. A better understanding of the *Hmgpi* transcriptional network will also improve culture methods for healthy blastocysts and for generating, maintaining and differentiating ES cells.

MATERIALS AND METHODS

Identification of the mouse *Hmgpi* gene by *in silico* analysis

Preimplantation-specific genes were identified based on global gene expression profiling of oocytes and preimplantation embryos (3,40) and expressed sequence tag (EST) frequencies in the Unigene database. SMART (19) was used for domain prediction analysis. Orthologous relationships between HMG family genes were identified from phylogenetic-tree amino acid sequences determined by a sequence distance method and the Neighbor Joining (NJ) algorithm (41) using Vector NTI software (Invitrogen, Carlsbad, CA, USA).

Collection and manipulation of embryos

Six- to 8-week-old B6D2F1 mice were superovulated by injecting 5 IU of pregnant-mare serum gonadotropin (PMS; Calbiochem, La Jolla, CA, USA) followed by 5 IU of human chorionic gonadotropin (HCG; Calbiochem) 48 h later. The Institutional Review Board of the National Research Institute for Child Health and Development, Japan granted ethics approval for embryo collection from the mice. Unfertilized eggs were harvested 18 h after the HCG injection by a standard published method (42), and the cumulus cells were removed by incubation in M2 medium (EmbryoMax M-2 Powdered Mouse Embryo Culture Medium; Millipore, Billerica, MA, USA) supplemented with 300 μg/ml hyaluronidase (Sigma-Aldrich, St Louis, MO, USA). The eggs were then thoroughly washed, selected for good morphology and collected. Fertilized eggs were also harvested from mated superovulated mice in the same way as unfertilized eggs and embryos with two pronuclei (PN) were collected to synchronize *in vitro* embryo development. Fertilized eggs were cultured in synthetic oviductal medium enriched with potassium (EmbryoMax KSOM Powdered Mouse Embryo Culture Medium; Millipore) at 37°C in an atmosphere of 95% air/5% CO_2. Cultured blastocysts were transferred into pseudopregnant recipients as described previously (42). We transferred 3.5 dpc blastocysts into the uteri of 2.5 dpc pseudopregnant ICR female mice. RNA interference experiments were carried out by microinjecting <10 pl (25 ng/μl) of oligonucleotides (siHmgpi and siControl) into the cytoplasm of zygotes. The optimal siRNAs were determined by testing different concentrations (5, 10, 25 and 50 ng/μl) of three siRNAs (PE Applied Biosystems, Foster City, CA, USA), resuspended and diluted with the microinjection buffer (Millipore). Their target sequences are listed in Supplementary Material, Table S3. More than 10 independent experiments were performed to study the effect of *Hmgpi* knockdown on preimplantation development and implantation.

Culture of ES cells and blastocyst outgrowth

A mouse ES cell line (B6/129ter/sv line) was first cultured for two passages on gelatin-coated culture dishes in the presence of leukemia inhibitory factor (LIF) to remove contaminating feeder cells. Cells were then seeded on gelatin-coated 6-well plates at a density of $1-2 \times 10^5$/well ($1-2 \times 10^4$/cm^2) and cultured for 3 days in complete ES medium: KnockOut DMEM (Invitrogen) containing 15% KnockOut Serum Replacement (KSR; Invitrogen), 2000 U/ml ESGRO (mLIF; Chemicon, Temecula, CA, USA), 0.1 mM non-essential amino acids, 2 mM GlutaMax (Invitrogen), 0.1 mM beta-mercaptoethanol (2-ME; Invitrogen) and penicillin/streptomycin (50 U/50 μg/ml; Invitrogen). Blastocyst outgrowth experiments were carried out according to a standard procedure (42). In brief, zona pellucidae of blastocysts at 3.5 dpc were removed using acidic Tyrode's solution (Sigma). The blastocysts were cultured individually in the ES medium on gelatinized chamber slides at 37°C in an atmosphere of 5% CO_2. The cultured cells were examined and photographed daily. Alkaline phosphatase activity was measured using a specific detection kit (Vector Laboratories, CA, USA) after 6 days in culture. Four independent experiments were performed.

Immunostaining of oocytes and preimplantation embryos

Samples were fixed in 4% paraformaldehyde (Wako Pure Chemical, Osaka, Japan) with 0.1% glutaraldehyde (Wako) in phosphate-buffered saline (PBS) for 10 min at room temperature (RT), and then permeabilized with 0.5% Triton X-100 (Sigma) in PBS for 30 min. Immunocytochemical staining was performed by incubating the fixed samples with primary antibodies for 60 min, followed by secondary antibodies for 60 min. A polyclonal antibody to mouse HMGPI was raised in rabbits against three synthesized peptides designed according to sequence specificity, homology between mouse and human HMGPI, antigenicity, hydrophilicity and synthetic suitability [(i) CIQGHHDGAQSSRQDFTD, (ii) CMSMSGG RSSKFGRTEQS, (iii) ESPRTVSSDMKFQGC; Medical & Biological Laboratories Co, Nagoya, Japan). The anti-HMPGI was used at 1:300 dilution, followed by Alexa Fluor 546 goat anti-rabbit IgG (Molecular Probes, Invitrogen) as the secondary antibody. The anti-Histone H2B antibody (Medical & Biological Laboratories Co, Nagoya, Japan) was used at 1:300 dilution as positive control of nuclear staining, followed by Alexa Fluor 488 goat anti-mouse IgG (Molecular Probes, Invitrogen) as the secondary antibody. Blastocysts were immunostained using a monoclonal anti-Oct4 antibody (mouse IgG2b isotype, 200 μg/ml; Santa Cruz Biotechnology, Santa Cruz, CA, USA), rabbit polyclonal anti-Nanog antibody (ReproCELL, Tokyo, Japan), mouse monoclonal anti-Cdx2 antibody (CELL MARQUE, Rocklin, CA, USA), mouse monoclonal anti-BrdU antibody (Santa Cruz) and rabbit monoclonal anti-active caspase 3 (Abcam) antibody, all diluted at 1:50–300. The appropriate secondary antibodies (IgG) were diluted at 1:300 and supplied by Molecular Probes/Invitrogen: goat anti-rabbit IgG conjugated with Alexa Fluor 546 and goat anti-mouse IgG(H + L) conjugated with Alexa Fluor 488. The cellular DNA (nuclei) was stained with 4′,6-diamidino-2-phenylindole (DAPI; Wako; diluted

1:300). The cells were then washed with PBS and viewed by laser confocal microscopy (LSM510, Zeiss). For HMGPI immunostaining, all samples were processed simultaneously. The laser power was adjusted so that the signal intensity was below saturation for the developmental stage that displayed the highest intensity and all subsequent images were scanned at that laser power. This allowed us to compare signal intensities for HMGPI expression at different developmental stages. The other molecules in blastocysts and outgrowth were viewed and imaged as for the HMGPI expression.

Immunocytochemistry of blastocyst outgrowths and ES cells

Cultured ES cells and blastocyst outgrowths were fixed with 4% paraformaldehyde for 10 min at 4°C, treated with 0.1% Triton X-100 (Sigma) in PBS for 15 min at RT, and then incubated for 30 min at RT in protein-blocking solution consisting of PBS supplemented with 5% normal goat serum (Dako, Glostrup, Denmark). The samples were then incubated overnight with the primary antibodies to OCT4, HMGPI, BrdU or active caspase 3 in PBS at 4°C. The cells were then extensively washed in PBS and incubated at RT with Alexa Fluor 488 goat anti-mouse IgG1 (anti-OCT4 and anti-BrdU antibodies, diluted 1:300; Molecular Probes) or Alexa Fluor 546 goat anti-rabbit IgG(H + L) (anti-HMGPI and anti-caspase 3 antibodies, diluted 1:300), and nuclei were counterstained with DAPI for 30 min. To prevent fading, cells were then mounted in Dako fluorescent mounting medium (Dako).

Incorporation of bromodeoxyuridine (BrdU)

E3.5 blastocysts and blastocyst outgrowths were cultured for 16 h in KSOM and ES medium, respectively, supplemented with 10 μM BrdU (Sigma). Samples were then fixed in 4% paraformaldehyde for 20 min, washed in PBS and then treated with 0.5 M HCl for 30 min.

RNA extraction and real-time quantitative reverse transcriptase (qRT)–PCR

Embryos for qRT–PCR analysis were collected at 18 h post-hCG and cultured as described above. They were harvested at 0.5, 1.25, 1.75, 2.25, 2.75 and 3.75 dpc to obtain fertilized eggs 2-cell, 4-cell, 8-cell, morula and blastocyst embryos, respectively. Three subsets of 10 and 50 synchronized and intact embryos were transferred in PBS supplemented with 3 mg/ml polyvinylpyrrolidone (PVP) and stored in liquid nitrogen. Total RNA from 10 and 50 embryos was extracted using the PicoPure RNA Isolation Kit (Arcturus, La Jolla, CA, USA). The reverse transcription reaction, primed with polyA primer, was performed using Superscript III reverse transcriptase (Invitrogen) following the manufacturer's instructions. Total RNA isolated was reverse transcribed in a 20 μl volume. The resulting cDNA was quantified by qRT–PCR analysis using the SYBR Green Realtime PCR Master Mix (Toyobo, Osaka, Japan) and ABI Prism 7700 Sequence Detection System (PE Applied Biosystems) as described previously (43). An amount of cDNA equivalent to 1/2 an embryo was used for each real-time PCR reaction with a minimum of three replicates, with no-RT and no-template controls for each gene. Data were normalized against *H2afz* by the ΔΔCt method (44). PCR primers for the genes of *Hmgpi, H2afz* and *Gapdh* were listed in Supplementary Material, Table S4. Calculations were automatically performed by ABI software (Applied BioSystems). For alpha-amanitin studies, fertilized eggs were first harvested at 18 h post-hCG, instead of eggs already advanced to the two-pronucleus stage. After 3 h of incubation, eggs that carried both male and female pronuclei were selected at 21 h post-hCG and randomly assigned to two experimental groups: with and without addition of alpha-amanitin to the culture medium. The eggs were further cultured in KSOM at 37°C in an atmosphere of 5% CO_2 until the specified time point (32, 43 and 54 h post-hCG). Embryos used for alpha-amanitin studies and RNA interference experiments were subjected to qRT–PCR as described for the normal preimplantation embryos.

Immunoblot analysis

Protein samples from embryos were solubilized in Sample Buffer Solution without 2-ME (Nacalai Tesque, Kyoto, Japan), resolved by NuPAGE Novex on Tris-acetate mini gels (Invitrogen), and transferred to Immobilon-P transfer membrane (Millipore). The membrane was soaked in protein blocking solution (Blocking One solution, Nacalai) for 30 min at RT before an overnight incubation at 4°C with primary antibody, also diluted in blocking solution. The membrane was then washed three times with TBST (Tris-buffered saline with 0.1% Tween-20), incubated with a horseradish peroxidase-conjugated secondary antibody (0.04 μg/ml) directed against the primary antibody for 60 min, and washed three times with TBST. The signal was detected by enhanced chemiluminescence (SuperSignal West Dura Extended Duration Substrate, Thermoscientific, Rockford, IL, USA) following the manufacturer's recommendations. The intensity of the band was quantified using NIH Image J software. Briefly, the signal was outlined and the mean intensity and background fluorescence were measured. The specific signal was calculated by dividing the band intensities for HMGPI by those for actin.

Statistical analysis

Differences between groups were evaluated statistically using Student's *t*-test or ANOVA, with *P*-values < 0.05 considered significant.

SUPPLEMENTARY MATERIAL

Supplementary Material is available at *HMG* online.

ACKNOWLEDGEMENTS

The authors would like to thank Dr Takashi Hiiragi for valuable advice and critical reading of the manuscript.

Conflict of Interest statement. The authors declare that there is no conflict of interest that would prejudice the impartiality of the scientific work.

FUNDING

This work was supported, in part, by Grants-in-Aid from the Japan Society for the Promotion of Science (19591911 to T.H., 21390456 to H.A.), by a National Grant-in-Aid from Japanese Ministry of Health, Labor, and Welfare (H21-001, H20-001 to T.H., H18-004 to H.A. and N.K.) and by a Grant-in-Aid from the Yamaguchi- Endocrine Organization to T.H. Funding to pay the Open Access publication charges for this article was provided by Grants-in-Aid for Young Scientists (B) (21791581 to M.Y.).

REFERENCES

1. DePamphilis, M.L., Kaneko, K.J. and Vassilev, A. (2002) Activation of zygotic gene expression in mammals. DePamphilis, M.L. (ed.), *Advances in Developmental Biology and Biochemistry*, Vol. 12, Elsevier Science, B.V.
2. Latham, K.E. and Schultz, R.M. (2001) Embryonic genome activation. *Front. Biosci.*, **6**, D748–D759.
3. Hamatani, T., Carter, M.G., Sharov, A.A. and Ko, M.S. (2004) Dynamics of global gene expression changes during mouse preimplantation development. *Dev. Cell.*, **6**, 117–131.
4. Takahashi, K. and Yamanaka, S. (2006) Induction of pluripotent stem cells from mouse embryonic and adult fibroblast cultures by defined factors. *Cell*, **126**, 663–676.
5. Hamatani, T., Yamada, M., Akutsu, H., Kuji, N., Mochimaru, Y., Takano, M., Toyoda, M., Miyado, K., Umezawa, A. and Yoshimura, Y. (2008) What can we learn from gene expression profiling of mouse oocytes? *Reproduction*, **135**, 581–592.
6. Ko, M.S., Kitchen, J.R., Wang, X., Threat, T.A., Hasegawa, A., Sun, T., Grahovac, M.J., Kargul, G.J., Lim, M.K., Cui, Y. *et al.* (2000) Large-scale cDNA analysis reveals phased gene expression patterns during preimplantation mouse development. *Development*, **127**, 1737–1749.
7. Okazaki, Y., Furuno, M., Kasukawa, T., Adachi, J., Bono, H., Kondo, S., Nikaido, I., Osato, N., Saito, R., Suzuki, H. *et al.* (2002) Analysis of the mouse transcriptome based on functional annotation of 60,770 full-length cDNAs. *Nature*, **420**, 563–573.
8. Solter, D., de Vries, W.N., Evsikov, A.V., Peaston, A.E., Chen, F.H. and Knowles, B.B. (2002) Fertilization and activation of the embryonic genome. Rossant, J. and Tam, P.P.L. (eds), *Mouse Development: Patterning, Morphogenesis, and Organogenesis.*, Academic Press, San Diego, pp. 5–19.
9. Wang, Q.T., Piotrowska, K., Ciemerych, M.A., Milenkovic, L., Scott, M.P., Davis, R.W. and Zernicka-Goetz, M. (2004) A genome-wide study of gene activity reveals developmental signaling pathways in the preimplantation mouse embryo. *Dev. Cell.*, **6**, 133–144.
10. Wang, S., Cowan, C.A., Chipperfield, H. and Powers, R.D. (2005) Gene expression in the preimplantation embryo: in-vitro developmental changes. *Reprod. Biomed. Online*, **10**, 607–616.
11. Zeng, F., Baldwin, D.A. and Schultz, R.M. (2004) Transcript profiling during preimplantation mouse development. *Dev. Biol.*, **272**, 483–496.
12. Choo, K.B., Chen, H.H., Cheng, W.T., Chang, H.S. and Wang, M. (2001) In silico mining of EST databases for novel pre-implantation embryo-specific zinc finger protein genes. *Mol. Reprod. Dev.*, **59**, 249–255.
13. Falco, G., Lee, S.L., Stanghellini, I., Bassey, U.C., Hamatani, T. and Ko, M.S. (2007) Zscan4: a novel gene expressed exclusively in late 2-cell embryos and embryonic stem cells. *Dev. Biol.*, **307**, 539–550.
14. Kanka, J. (2003) Gene expression and chromatin structure in the pre-implantation embryo. *Theriogenology*, **59**, 3–19.
15. Schultz, R.M. and Worrad, D.M. (1995) Role of chromatin structure in zygotic gene activation in the mammalian embryo. *Semin. Cell Biol.*, **6**, 201–208.
16. Thompson, E.M., Legouy, E. and Renard, J.P. (1998) Mouse embryos do not wait for the MBT: chromatin and RNA polymerase remodeling in genome activation at the onset of development. *Dev. Genet.*, **22**, 31–42.
17. Stros, M., Launholt, D. and Grasser, K.D. (2007) The HMG-box: a versatile protein domain occurring in a wide variety of DNA-binding proteins. *Cell. Mol. Life Sci.*, **64**, 2590–2606.
18. Zhang, Q. and Wang, Y. (2008) High mobility group proteins and their post-translational modifications. *Biochim. Biophys. Acta*, **1784**, 1159–1166.
19. Schultz, J., Milpetz, F., Bork, P. and Ponting, C.P. (1998) SMART, a simple modular architecture research tool: identification of signaling domains. *Proc. Natl Acad. Sci. USA*, **95**, 5857–5864.
20. Mamo, S., Gal, A.B., Bodo, S. and Dinnyes, A. (2007) Quantitative evaluation and selection of reference genes in mouse oocytes and embryos cultured in vivo and in vitro. *BMC Dev. Biol.*, **7**, 14.
21. Hock, R., Furusawa, T., Ueda, T. and Bustin, M. (2007) HMG chromosomal proteins in development and disease. *Trends Cell Biol.*, **17**, 72–79.
22. Svarcova, O., Dinnyes, A., Polgar, Z., Bodo, S., Adorjan, M., Meng, Q. and Maddox-Hyttel, P. (2009) Nucleolar re-activation is delayed in mouse embryos cloned from two different cell lines. *Mol. Reprod. Dev.*, **76**, 132–141.
23. Sanij, E., Poortinga, G., Sharkey, K., Hung, S., Holloway, T.P., Quin, J., Robb, E., Wong, L.H., Thomas, W.G., Stefanovsky, V. *et al.* (2008) UBF levels determine the number of active ribosomal RNA genes in mammals. *J. Cell Biol.*, **183**, 1259–1274.
24. Stefanovsky, V.Y., Pelletier, G., Hannan, R., Gagnon-Kugler, T., Rothblum, L.I., Moss, T., Bazett-Jones, D.P. and Crane-Robinson, C. (2001) An immediate response of ribosomal transcription to growth factor stimulation in mammals is mediated by ERK phosphorylation of UBF DNA looping in the RNA polymerase I enhancesome is the result of non-cooperative in-phase bending by two UBF molecules. *Mol. Cell.*, **8**, 1063–1073.
25. Stefanovsky, V.Y., Pelletier, G., Bazett-Jones, D.P., Crane-Robinson, C. and Moss, T. (2001) DNA looping in the RNA polymerase I enhancesome is the result of non-cooperative in-phase bending by two UBF molecules. *Nucleic Acids Res.*, **29**, 3241–3247.
26. Mais, C., Wright, J.E., Prieto, J.L., Raggett, S.L. and McStay, B. (2005) UBF-binding site arrays form pseudo-NORs and sequester the RNA polymerase I transcription machinery. *Genes Dev.*, **19**, 50–64.
27. Falciola, L., Spada, F., Calogero, S., Langst, G., Voit, R., Grummt, I. and Bianchi, M.E. (1997) High mobility group 1 protein is not stably associated with the chromosomes of somatic cells. *J. Cell Biol.*, **137**, 19–26.
28. Bonaldi, T., Talamo, F., Scaffidi, P., Ferrera, D., Porto, A., Bachi, A., Rubartelli, A., Agresti, A. and Bianchi, M.E. (2003) Monocytic cells hyperacetylate chromatin protein HMGB1 to redirect it towards secretion. *EMBO J.*, **22**, 5551–5560.
29. Wang, H., Bloom, O., Zhang, M., Vishnubhakat, J.M., Ombrellino, M., Che, J., Frazier, A., Yang, H., Ivanova, S., Borovikova, L. *et al.* (1999) HMG-1 as a late mediator of endotoxin lethality in mice. *Science*, **285**, 248–251.
30. Cui, X.S., Shen, X.H. and Kim, N.H. (2008) High mobility group box 1 (HMGB1) is implicated in preimplantation embryo development in the mouse. *Mol. Reprod. Dev.*, **75**, 1290–1299.
31. Payer, B., Saitou, M., Barton, S.C., Thresher, R., Dixon, J.P., Zahn, D., Colledge, W.H., Carlton, M.B., Nakano, T. and Surani, M.A. (2003) Stella is a maternal effect gene required for normal early development in mice. *Curr. Biol.*, **13**, 2110–2117.
32. Gurtu, V.E., Verma, S., Grossmann, A.H., Liskay, R.M., Skarnes, W.C. and Baker, S.M. (2002) Maternal effect for DNA mismatch repair in the mouse. *Genetics*, **160**, 271–277.
33. Hock, R., Scheer, U. and Bustin, M. (1998) Chromosomal proteins HMG-14 and HMG-17 are released from mitotic chromosomes and imported into the nucleus by active transport. *J. Cell Biol.*, **143**, 1427–1436.
34. Mitsui, K., Tokuzawa, Y., Itoh, H., Segawa, K., Murakami, M., Takahashi, K., Maruyama, M., Maeda, M. and Yamanaka, S. (2003) The homeoprotein Nanog is required for maintenance of pluripotency in mouse epiblast and ES cells. *Cell*, **113**, 631–642.
35. Kim, J.B., Zaehres, H., Wu, G., Gentile, L., Ko, K., Sebastiano, V., Arauzo-Bravo, M.J., Ruau, D., Han, D.W., Zenke, M. *et al.* (2008)

Pluripotent stem cells induced from adult neural stem cells by reprogramming with two factors. *Nature*, **454**, 646–650.
36. Levine, A.J. and Brivanlou, A.H. (2006) GDF3, a BMP inhibitor, regulates cell fate in stem cells and early embryos. *Development*, **133**, 209–216.
37. Takahashi, K., Mitsui, K. and Yamanaka, S. (2003) Role of ERas in promoting tumour-like properties in mouse embryonic stem cells. *Nature*, **423**, 541–545.
38. Nimura, K., Ishida, C., Koriyama, H., Hata, K., Yamanaka, S., Li, E., Ura, K. and Kaneda, Y. (2006) Dnmt3a2 targets endogenous Dnmt3L to ES cell chromatin and induces regional DNA methylation. *Genes Cells*, **11**, 1225–1237.
39. Arima, T., Hata, K., Tanaka, S., Kusumi, M., Li, E., Kato, K., Shiota, K., Sasaki, H. and Wake, N. (2006) Loss of the maternal imprint in Dnmt3Lmat-/- mice leads to a differentiation defect in the extraembryonic tissue. *Dev. Biol.*, **297**, 361–373.
40. Pan, H., O'Brien, M.J., Wigglesworth, K., Eppig, J.J. and Schultz, R.M. (2005) Transcript profiling during mouse oocyte development and the effect of gonadotropin priming and development in vitro. *Dev. Biol.*, **286**, 493–506.
41. Saitou, N. and Nei, M. (1987) The neighbor-joining method: a new method for reconstructing phylogenetic trees. *Mol. Biol. Evol.*, **4**, 406–425.
42. Nagy, A., Gertsenstein, M., Vintersten, K. and Behringer, R. (2003) *Manipulating the Mouse Embryo: A Laboratory Manual.*, 3rd edn. Cold Spring Harbor Laboratory.
43. Hamatani, T., Falco, G., Carter, M.G., Akutsu, H., Stagg, C.A., Sharov, A.A., Dudekula, D.B., VanBuren, V. and Ko, M.S. (2004) Age-associated alteration of gene expression patterns in mouse oocytes. *Hum. Mol. Genet.*, **13**, 2263–2278.
44. Falco, G., Stanghellini, I. and Ko, M.S. (2006) Use of Chuk as an internal standard suitable for quantitative RT-PCR in mouse preimplantation embryos. *Reprod. Biomed. Online*, **13**, 394–403.

Journal of Reproduction and Development, Vol. 56, No. 1, 2010

SRD Young Investigator Award 2009

Induction of Oocyte Maturation by Hyaluronan-CD44 Interaction in Pigs

Masaki YOKOO[1], Naoko KIMURA[2] and Eimei SATO[3]

[1]Laboratory of Animal Reproduction, Faculty of Bioresource Sciences, Akita Prefectural University, Minamiakita-gun 010-0444, [2]Laboratory of Animal Reproduction, Faculty of Agriculture, Yamagata University, Tsuruoka 997-8555 and [3]Laboratory of Animal Reproduction, Graduate School of Agricultural Science, Tohoku University, Sendai 981-8555, Japan

Abstract. In most mammals, the oocyte is surrounded with compact multilayers of cumulus cells; these form cumulus-oocyte complexes (COCs). During oocyte maturation, the COCs dramatically expand and this is termed "cumulus expansion". We have previously demonstrated that cumulus expansion is the result of hyaluronan synthesis and accumulation in the extracellular space between cumulus cells in the COCs and that hyaluronan accumulation within the COCs affects oocyte maturation. We have also demonstrated that CD44, the principal hyaluronan receptor, is expressed in the COCs during cumulus expansion and that the interaction between hyaluronan and CD44 appears to be closely related to gap junctional communication of the COCs during the process of meiotic resumption. Based on our previous studies, we review herein that the physiological significance and the molecular mechanism of cumulus expansion for porcine oocyte maturation.

Key words: CD44, Cumulus expansion, Gap junction, Hyaluronan, Oocyte maturation

(J. Reprod. Dev. 56: 15–19, 2010)

In nearly all mammals, the oocyte is surrounded by compact multilayers of cumulus cells that form cumulus-oocyte complexes (COCs). During oocyte maturation, the COCs expand dramatically; this phenomenon is termed "cumulus expansion" and occurs after the pre-ovulatory surge of gonadotropins. It has been reported that cumulus expansion supports dissociation from the follicle wall and the expulsion of the oocyte through the ruptured follicle wall during ovulation. In addition to these effects, it has been reported that the expansion of COCs is essential for fertilization and the developmental potential of early embryos [1, 2]. Therefore, the degree of cumulus expansion is often cited as a major indicator in the selection of oocytes for *in vitro* fertilization (IVF) protocols [3–5]. Considering these observations, it is clear that an understanding of the physiological significance of cumulus expansion is important to the study of the developmental competence of mammalian oocytes that are matured and fertilized *in vitro*. Therefore, based on our previous studies, we describe herein the physiological significance and the molecular mechanism of cumulus expansion in porcine oocyte maturation.

Effects of Cumulus Expansion on Oocyte Maturation

Many researchers have documented that the formation of the COC matrix during cumulus expansion is characterized by the intercellular deposition of hyaluronan secreted from cumulus cells [6–8]. We first investigated whether the induction of cumulus expansion was due to the synthesis of hyaluronan during porcine oocyte maturation. COCs were cultured in maturation medium with or without 6-diazo-5-oxo-l-norleucine (DON; an inhibitor of hyaluronan synthesis) for 48 h. The degree of cumulus expansion increased gradually until 48 h in culture in the control medium. When the COCs were cultured with DON, they showed no evidence of cumulus expansion during the culture period. In addition, a remarkable accumulation of hyaluronan was confirmed in porcine expanded COCs by the immunostaining method, but hyaluronan accumulation was completely inhibited by treatment with DON (Fig. 1). These results indicate that the expanded cumulus mass of porcine COCs consists mainly of hyaluronan [9, 10].

Generally, serum and follicular fluid contain a factor(s) that stabilizes the hyaluronan-rich matrix. Previous studies have demonstrated that the inter-α-trypsin inhibitor (ITI) family plays an important role in the formation of the extracellular matrix of which hyaluronan is the predominant component [11]. Proteins of the ITI family are composed of a common light chain called "bikunin" and either one or two heavy polypeptide chains (HCs). In addition, serum-derived hyaluronan-associated proteins (SHAPs) have been isolated from the hyaluronan-rich extracellular matrix of mouse dermal fibroblasts cultured in the presence of serum [12], and these proteins were identical to the HCs of ITI [13]. It has been reported that the formation of a bond between SHAP and hyaluronan is also important for the stabilization of the hyaluronan-rich matrix [14, 15]. In our previous study, we documented that SHAPs were also present in porcine follicular fluid and serum as a single protein band at 70 kDa (Yokoo *et al.* unpublished data). In pigs, it has been reported that there is no apparent barrier to the transfer of SHAPs from the blood to the follicle [16]. Therefore, it is believed that SHAPs present in porcine follicular fluid are derived from serum.

Received: September 29, 2009
Accepted: September 29, 2009

Correspondence: M. Yokoo (e-mail: myokoo@akita-pu.ac.jp)

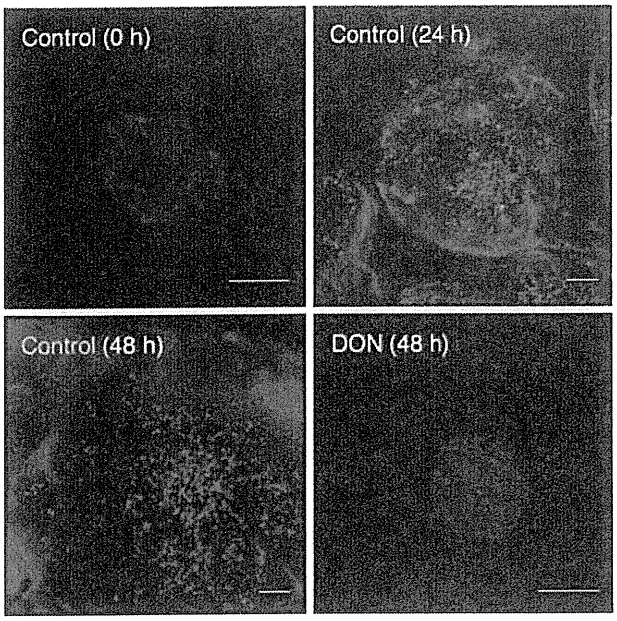

Fig. 1. Localization of hyaluronan in porcine cumulus-oocyte complexes (COCs) as detected by immunofluorescence using biotinylated hyaluronan-binding protein. Green=hyaluronan; red=nuclear; bars=100 μm.

Moreover, we demonstrated that the immunodepletion of SHAPs from follicular fluid produced not only incomplete cumulus expansion but also a decline in the oocyte maturation rates in a manner dependent on the antibody concentration against SHAPs. These results suggest that the retention and stabilization of hyaluronan within the COCs by the formation of the hyaluronan-SHAP complex during cumulus expansion is necessary for porcine oocyte maturation.

Expression of Hyaluronan-CD44 Interaction in COCs

Hyaluronan, which is the main component of cumulus expansion, is a linear glycosaminoglycan that is a high-molecular-weight polymer with repeating disaccharides linked by β 1–3 and β 1–4 glycosidic bonds. Despite its structural simplicity, hyaluronan is a biologically important biopolymer that is widely distributed in the extracellular matrix of connective tissues in the body. It plays important roles in diverse processes such as wound repair, cell motility, and cancer metastasis. Unlike others of the glycosaminoglycan family, hyaluronan is neither sulfated nor linked to a core protein. Hence, hyaluronan needs hyaluronan binding protein(s) for its biological functions. To obtain information regarding hyaluronan binding protein(s) during cumulus expansion, we investigated their expression in COCs during oocyte maturation by ligand blotting analysis with fluorescein isothiocyanate (FITC)-labeled hyaluronan. Interestingly, an 85-kDa hyaluronan binding protein was detected only in expanded COCs after maturation. Using immunoprecipitation assay, we showed that this protein was identical to CD44 [17].

CD44 is the principal cell-surface receptor for extracellular matrix hyaluronan and exists in a number of isoforms with different molecular sizes (approximately 80–250 kDa) on a wide variety of cell types [18–21]. It has been reported that the function of hyaluronan via CD44 is responsible for cell-to-cell and cell-to-extracellular matrix interactions [22], inhibition of apoptosis [23], augmentation of tumor cell motility and metastasis [24], and stimulation of lymphocytes [25]. Additionally, previous studies have indicated that the hyaluronan-CD44 interaction may influence fertility and the quality of oocytes [26, 27]. However, the role of CD44 in oocyte maturation remains poorly understood. To elucidate the role of hyaluronan-CD44 interaction in oocyte maturation, we examined the maturation-promoting factor (MPF) activity and the germinal vesicle breakdown (GVBD) rates in the COCs cultured in maturation medium containing with anti-CD44 antibody, which has been used for inhibition of hyaluronan binding [28, 29]. A low level of MPF activity was noted in oocytes from the COCs immediately after collection from follicles. After 24 h in culture, the MPF activity and the GVBD rates in oocytes cultured in the drug-free medium significantly increased compared to those of cumulus-oocyte complexes before culture. However, exposure of the COCs to anti-CD44 antibody during 24 h of culture significantly suppressed MPF activity and GVBD rates compared to those of the COCs cultured in the drug-free medium for 24 h (Table 1 and Table 2). Thus, these results clearly show that the hyaluronan-CD44 interaction is required for meiotic resumption in the oocyte maturation process.

We next examined the difference between the molecular size of CD44 expressed in the COCs matured *in vitro* and those matured *in vivo* [30]. The COCs matured *in vitro* showed bands of CD44 ranging from 81 to 88 kDa. However, the CD44 band in the *in vivo*-matured COCs was 73–83 kDa in size; thus, the size of the CD44 in the COCs matured *in vivo* was clearly smaller than the band of CD44 in the COCs matured *in vitro*. The amino acid sequence of CD44 predicts a polypeptide of <40 kDa, which contrasts with its apparent size on gel electrophoresis (approximately 80–250 kDa). This difference appears to be the result of extensive glycosylation of the extracellular domain [31]. It has been reported that CD44 glycosylation has been implicated in the regulation and function of CD44-mediated cell binding for hyaluronan [19]. Notably, Katoh *et al.* [32] reported that the terminal sialic acids on CD44 have an inhibitory effect on hyaluronan binding ability of CD44. Our results clearly demonstrated that the treatment with sialidase reduced the size of CD44 in the COCs matured *in vitro*, the size of which was not significantly different from that of the COCs matured *in vivo*. This evidence indicates the possibility that interaction between hyaluronan and CD44 during *in vitro* maturation may not be sufficient for oocyte maturation compared to that *in vivo*. In general, oocytes matured *in vitro* have a reduced capacity to be fertilized and a higher rate of abnormal fertilization and development as compared to their *in vivo* counterparts. In pigs, although oocytes matured *in vitro* can be penetrated by spermatozoa under appropriate conditions, *in vitro* maturation is associated with low rates of pronuclear formation and a high incidence of polyspermy [33]. Sun *et al.* [34] demonstrated that the rates of embryo development rates of *in vitro*-matured and fertilized COCs

Table 1. Effects of 6-diazo-5-oxo-norleucine (DON) and anti-CD44 antibody on maturation-promoting factor (MPF) activity in porcine oocytes

	Relative MPF activity (0 h=1)			
	0 h	6 h	12 h	24 h
Control	1^{a}	1.09 ± 0.04^{a}	1.94 ± 0.10^{c}	5.87 ± 0.44^{d}
DON	1^{a}	1.32 ± 0.12^{a}	0.99 ± 0.08^{a}	2.51 ± 0.43^{b}
Anti-CD-44	1^{a}	1.01 ± 0.08^{a}	1.00 ± 0.01^{a}	2.16 ± 0.15^{b}

Cumulus-oocyte complexes were cultured for 0, 6, 12 or 24 h with 1.0 mM DON or 5.0 mg/ml anti-CD44 antibody. Data are expressed as fold increases of MPF activity in oocytes just after collection from follicles, defined as 1. Experiments were replicated four times at least. Data represent mean ± standard deviation (SD). Different superscripts denote significant differences ($P<0.05$).

Table 2. Effects of 6-diazo-5-oxo-norleucine (DON) and anti-CD44 antibody on germinal vesicle breakdown (GVBD)

	Rate of GVBD (%)			
	0 h	6 h	12 h	24 h
Control	0^{a}	2.5 ± 2.5^{a}	4.8 ± 4.8^{a}	63.8 ± 2.4^{c}
DON	0^{a}	2.4 ± 2.4^{a}	4.5 ± 4.5^{a}	19.0 ± 2.1^{b}
Anti-CD44	0^{a}	2.1 ± 2.1^{a}	6.8 ± 6.8^{a}	13.3 ± 7.0^{b}

Cumulus-oocyte complexes were cultured for 0, 6, 12 or 24 h with 1.0 mM DON or 5.0 mg/ml anti-CD44 antibody. Experiments were replicated three times at least. Data represent mean ± SD. Different superscripts denote significant differences ($P<0.05$).

is significantly lower than that observed *in vivo*. Based on these observations, we speculate that the insufficient interaction of hyaluronan-CD44 during cumulus expansion *in vitro* may cause inferior fertilization and developmental capacities in oocytes compared to those matured *in vivo*.

Molecular Mechanism of Hyaluronan-CD44 Interaction for Oocyte Maturation

Since our findings suggested that the hyaluronan-CD44 interaction is involved in the induction of meiotic resumption, it was thought that CD44 was expressed in/on the oocytes. However, CD44 has been shown to be localized in cumulus cells, not in the oocyte, of the COCs by using reverse-transcription polymerase chain reaction (RT-PCR), western blotting, and immnunohistological staining [17, 35, 36]. Considering these results, we conclude that the hualuronan-CD44 interaction might function to promote the meiotic resumption of porcine oocytes through the cumulus cells.

Generally, the coordination of function between the oocyte and cumulus cells is mediated by cell-cell communication via gap junctions [37]. Early studies have shown that oocyte growth and development are strictly dependent upon the supply of nutrients transmitted from the follicle cells [38, 39]. Later studies have demonstrated that the meiotic maturation of oocytes is also subject to regulation by the somatic compartment of the ovarian follicle. MPF activation at the onset of meiotic resumption is inhibited by intra-oocyte cAMP, which is transferred from cumulus cells via gap junctional communication within COCs [37]. Interruption of gap junctions in the COCs, which occurs in response to the preovulatory surge of gonadotropins, leads to a drop in the intra-oocyte concentration of cAMP, followed by MPF activation and meiotic resumption [40–42]. We demonstrated that the reduction of the intra-oocyte cAMP concentration was suppressed by the inhibition of the interaction between hyaluronan and CD44 (Yokoo *et al.* unpublished data). This result supports the concept that hyaluronan-CD44 interaction is involved in the regulation of gap junctional communication and the termination of the flux of cAMP flux from cumulus cells to oocytes.

Gap junctions are specialized regions in closely opposed membranes of neighboring cells that allow cells to exchange small molecules, thus coordinating their activities. Each gap junction channel comprises two symmetrical hemispheres (termed "connexons") derived from two neighboring cells. The connexon comprises a hexagonal arrangement of six subunits of a protein named "connexin" (Cx). Connexins are encoded by members of a multigene family; they are defined by their molecular weight and share high homology. At present, at least 15 connexin genes have been reported in mammals and 7 genes (*Cx26, Cx30, Cx32, Cx37, Cx43, Cx45 and Cx60*) have been identified in the ovary. We examined the effects of the hyaluronan-CD44 interaction on the expression of Cx43, which is the most abundant Cx found in the ovarian follicle and in the COCs. Exposure of COCs to DON and anti-CD44 antibody had no effect on the expression of total Cx43 in the COCs. Conversely, these treatments significantly inhibited the tyrosine-phosphorylation of Cx43 in the COCs (Fig. 2). Previous studies have shown that a tyrosine kinase, such as $pp60^{Src}$, induces the tyrosine phosphorylation of Cx43 and inhibits intercellular junctional communication [43–47]. Therefore, it is suggested that hyaluronan-CD44 interaction controls the inhibition of Cx43 gap junctional communication in COCs. These findings strongly suggest that the hyaluronan-CD44 interaction during cumulus

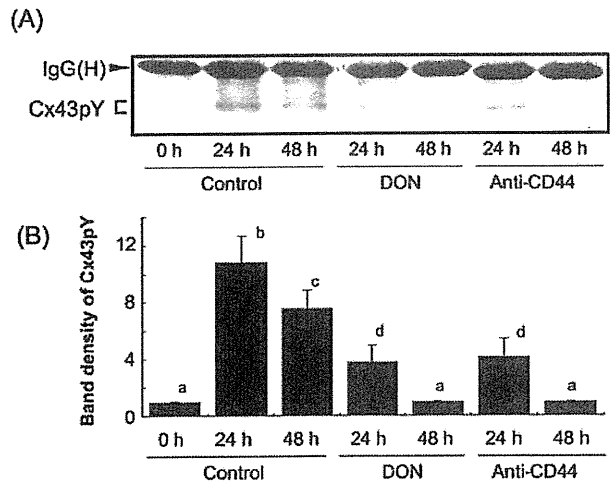

Fig. 2. Effects of 6-diazo-5-oxo-norleucine (DON) and anti-CD44 antibody on expression of Cx43. The cumulus-oocyte complexes (COCs) were cultured with 1.0 mM DON or 5.0 μg/ml anti-CD44 antibody. (A) Detection of tyrosine-phosphorylated Cx43 (Cx43pY). The extracts immunoprecipitated with anti-Cx43 antibody were probed with anti-phosphotyrosine antibody. Arrowhead means the band of heavy chain of immunoglobulin (IgG (H)). (B) Densitometric analysis of (A). Different superscripts denote significant differences ($P<0.05$). Data represent mean ± SD.

expansion induces disruption of the Cx43 gap junction in the COCs, inhibits the transport of cAMP from cumulus cells into oocytes, and leads to activation of MPF and meiotic resumption of oocytes (Fig. 3).

Concluding Remarks

Oocyte maturation is roughly divided into two types: nuclear maturation and cytoplasmic maturation. We have described herein the hyaluronan-CD44 interaction during cumulus expansion that concurrently controls the occurrence of meiotic resumption through the disruption of gap junctions in COCs. It has been demonstrated that volumetric expansion of COCs actively correlates, at least in the pig, with the progress of nuclear maturation. Although details of the mechanism controlling cytoplasmic maturation in mammals are still unclear, we believe that our findings as described here shed some light on the understanding of the cytoplasmic maturation process.

Recently, pigs have become increasingly important in the field of biomedical research and interest has grown in the use of transgenic pigs as potential xenograph donors. As most attempts to produce transgenic pigs by nuclear transfer/cloning techniques or pronuclear microinjection have used matured oocytes and early embryos, respectively, it is becoming more important to produce large numbers of developmentally competent oocytes and embryos. The developmental competence of porcine oocytes that are matured and fertilized *in vitro* has been enhanced by mimicking the active communication between the oocyte and follicular cells. Therefore,

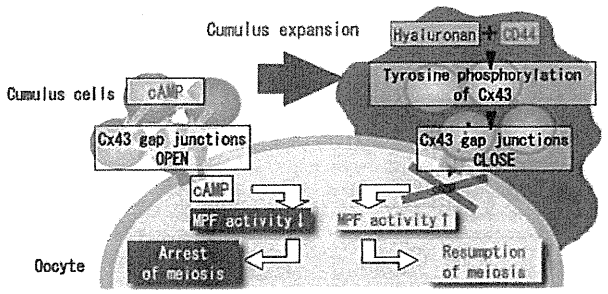

Fig. 3. Schematic representation of the oocyte maturation mechanism in the pig.

elucidation of the molecular mechanisms of oocyte maturation will enable substantial improvement of the quality of oocytes and embryos cultured *in vitro*.

During the past decade, new reproduction biotechnology based on molecular genetics, molecular biology, and embryology has rapidly developed. These techniques should enable us to increase the production of domestic animals. We now need to define issues and further develop the study of animal reproduction. The objective of our ongoing studies is to investigate in more detail the molecular mechanism of mammalian oocyte maturation and to develop an artificial technique for oocyte maturation *in vitro*.

Acknowledgements

We are very grateful to Drs H Sasada and H Matsumoto for their support and helpful discussions. We thank the undergraduate and graduate students in Tohoku University for their assistance. Finally, we wish to thank all of the members of the Society for Reproduction and Development for conferring the SRD Young Investigator Award 2009 on our study.

References

1. **Chen L, Russell PT, Larsen WJ.** Functional significance of cumulus expansion in the mouse: roles for the preovulatory synthesis of hyaluronic acid within the cumulus mass. *Mol Reprod Dev* 1993; 34: 87–93.
2. **Hess KA, Chen L, Larsen WJ.** Inter-alpha-inhibitor binding to hyaluronan in the cumulus extracellular matrix is required for optimal ovulation and development of mouse oocytes. *Biol Reprod* 1999; 61: 436–443.
3. **Qian Y, Shi WQ, Ding JT, Sha JH, Fan BQ.** Predictive value of the area of expanded cumulus mass on development of porcine oocytes matured and fertilized *in vitro*. *J Reprod Dev* 2003; 49: 167–174.
4. **Somfai T, Kikuchi K, Onishi A, Iwamoto M, Fuchimoto D, Papp AB, Sato E, Nagai T.** Relationship between the morphological changes of somatic compartment and the kinetics of nuclear and cytoplasmic maturation of oocytes during *in vitro* maturation of porcine follicular oocytes. *Mol Reprod Dev* 2004; 68: 484–491.
5. **Yang LS, Kadam AL, Koide SS.** Identification of a cAMP-dependent protein kinase in bovine and human follicular fluids. *Biochem Mol Biol Int* 1993; 31: 521–525.
6. **Camaioni A, Salustri A, Yanagishita M, Hascall VC.** Proteoglycans and proteins in the extracellular matrix of mouse cumulus cell-oocyte complexes. *Arch Biochem Biophys* 1996; 325: 190–198.
7. **Salustri A, Yanagishita M, Hascall VC.** Synthesis and accumulation of hyaluronic acid and proteoglycans in the mouse cumulus cell-oocyte complex during follicle-stimulating hormone-induced mucification. *J Biol Chem* 1989; 264: 13840–13847.
8. **Eppig JJ.** FSH stimulates hyaluronic acid synthesis by oocyte-cumulus cell complexes from mouse preovulatory follicles. *Nature* 1979; 281: 483–484.

9. **Nakayama T, Inoue M, Sato E.** Effect of oocytectomy on glycosaminoglycan composition during cumulus expansion of porcine cumulus-oocyte complexes cultured *in vitro*. *Biol Reprod* 1996; 55: 1299–1304.
10. **Yokoo M, Kimura N, Abe H, Sato E.** Influence of hyaluronan accumulation during cumulus expansion on *in vitro* porcine oocyte maturation. *Zygote* 2008; 16: 309–314.
11. **Enghild JJ, Salvesen G, Hefta SA, Thogersen IB, Rutherfurd S, Pizzo SV.** Chondroitin 4-sulfate covalently cross-links the chains of the human blood protein pre-alpha-inhibitor. *J Biol Chem* 1991; 266: 747–751.
12. **Yoneda M, Suzuki S, Kimata K.** Hyaluronic acid associated with the surfaces of cultured fibroblasts is linked to a serum-derived 85-kDa protein. *J Biol Chem* 1990; 265: 5247–5257.
13. **Huang L, Yoneda M, Kimata K.** A serum-derived hyaluronan-associated protein (SHAP) is the heavy chain of the inter alpha-trypsin inhibitor. *J Biol Chem* 1993; 268: 26725–26730.
14. **Yingsung W, Zhuo L, Morgelin M, Yoneda M, Kida D, Watanabe H, Ishiguro N, Iwata H, Kimata K.** Molecular heterogeneity of the SHAP-hyaluronan complex. Isolation and characterization of the complex in synovial fluid from patients with rheumatoid arthritis. *J Biol Chem* 2003; 278: 32710–32718.
15. **Kida D, Yoneda M, Miyaura S, Ishimaru T, Yoshida Y, Ito T, Ishiguro N, Iwata H, Kimata K.** The SHAP-HA complex in sera from patients with rheumatoid arthritis and osteoarthritis. *J Rheumatol* 1999; 26: 1230–1238.
16. **Nagyova E, Camaioni A, Prochazka R, Salustri A.** Covalent transfer of heavy chains of inter-alpha-trypsin inhibitor family proteins to hyaluronan in *in vivo* and *in vitro* expanded porcine oocyte-cumulus complexes. *Biol Reprod* 2004; 71: 1838–1843.
17. **Yokoo M, Miyahayashi Y, Naganuma T, Kimura N, Sasada H, Sato E.** Identification of hyaluronic acid-binding proteins and their expressions in porcine cumulus-oocyte complexes during *in vitro* maturation. *Biol Reprod* 2002; 67: 1165–1171.
18. **Aruffo A, Stamenkovic I, Melnick M, Underhill CB, Seed B.** CD44 is the principal cell surface receptor for hyaluronate. *Cell* 1990; 61: 1303–1313.
19. **Bartolazzi A, Nocks A, Aruffo A, Spring F, Stamenkovic I.** Glycosylation of CD44 is implicated in CD44-mediated cell adhesion to hyaluronan. *J Cell Biol* 1996; 132: 1199–1208.
20. **Lesley J, Hyman R, Kincade PW.** CD44 and its interaction with extracellular matrix. *Adv Immunol* 1993; 54: 271–335.
21. **Underhill C.** CD44: the hyaluronan receptor. *J Cell Sci* 1992; 103 (Pt 2): 293–298.
22. **Aruffo A.** CD44: one ligand, two functions. *J Clin Invest* 1996; 98: 2191–2192.
23. **Kaneko T, Saito H, Toya M, Satio T, Nakahara K, Hiroi M.** Hyaluronic acid inhibits apoptosis in granulosa cells via CD44. *J Assist Reprod Genet* 2000; 17: 162–167.
24. **Thomas GJ, Speight PM.** Cell adhesion molecules and oral cancer. *Crit Rev Oral Biol Med* 2001; 12: 479–498.
25. **Lesley J, Hyman R, English N, Catterall JB, Turner GA.** CD44 in inflammation and metastasis. *Glycoconj J* 1997; 14: 611–622.
26. **Schoenfelder M, Einspanier R.** Expression of hyaluronan synthases and corresponding hyaluronan receptors is differentially regulated during oocyte maturation in cattle. *Biol Reprod* 2003; 69: 269–277.
27. **Ohta N, Saito H, Kuzumaki T, Takahashi T, Ito MM, Saito T, Nakahara K, Hiroi M.** Expression of CD44 in human cumulus and mural granulosa cells of individual patients in *in-vitro* fertilization programmes. *Mol Hum Reprod* 1999; 5: 22–28.
28. **Yokoo M, Kimura N, Shimizu T, Naganuma T, Matsumoto H, Sasada H, Sato E.** Induction of porcine oocyte maturation by hyaluronan-CD44 system. *J Fertil Implant* 2003; 20: 33–36.
29. **Yokoo M, Sato E.** Cumulus-oocyte complex interactions during oocyte maturation. *Int Rev Cytol* 2004; 235: 251–291.
30. **Yokoo M, Tientha P, Kimura N, Niwa K, Sato E, Rodriguez-Martinez H.** Localisation of the hyaluronan receptor CD44 in porcine cumulus cells during *in vivo* and *in vitro* maturation. *Zygote* 2002; 10: 317–326.
31. **Borland G, Ross JA, Guy K.** Forms and functions of CD44. *Immunology* 1998; 93: 139–148.
32. **Katoh S, Miyagi T, Taniguchi H, Matsubara Y, Kadota J, Tominaga A, Kincade PW, Matsukura S, Kohno S.** Cutting edge: an inducible sialidase regulates the hyaluronic acid binding ability of CD44-bearing human monocytes. *J Immunol* 1999; 162: 5058–5061.
33. **Hunter MG.** Oocyte maturation and ovum quality in pigs. *Rev Reprod* 2000; 5: 122–130.
34. **Sun QY, Lai L, Bonk A, Prather RS, Schatten H.** Cytoplasmic changes in relation to nuclear maturation and early embryo developmental potential of porcine oocytes: effects of gonadotropins, cumulus cells, follicular size, and protein synthesis inhibition. *Mol Reprod Dev* 2001; 59: 192–198.
35. **Kimura N, Konno Y, Miyoshi K, Matsumoto H, Sato E.** Expression of hyaluronan synthases and CD44 messenger RNAs in porcine cumulus-oocyte complexes during *in vitro* maturation. *Biol Reprod* 2002; 66: 707–717.
36. **Tienthai P, Yokoo M, Kimura N, Heldin P, Sato E, Rodriguez-Martinez H.** Immunohistochemical localization and expression of the hyaluronan receptor CD44 in the epithelium of the pig oviduct during oestrus. *Reproduction* 2003; 125: 119–132.
37. **Dekel N.** Spatial relationship of follicular cells in the control of the meiosis. *In*: Heseltine FP (ed.), Meotic Inhibition: Molecular Control of Meiosis: Alan R Liss; 1988: 87–101.
38. **Brower PT, Schultz RM.** Intercellular communication between granulosa cells and mouse oocytes: existence and possible nutritional role during oocyte growth. *Dev Biol* 1982; 90: 144–153.
39. **Eppig JJ.** A comparison between oocyte growth in coculture with granulosa cells and oocytes with granulosa cell-oocyte junctional contact maintained *in vitro*. *J Exp Zool* 1979; 209: 345–353.
40. **Isobe N, Maeda T, Terada T.** Involvement of meiotic resumption in the disruption of gap junctions between cumulus cells attached to pig oocytes. *J Reprod Fertil* 1998; 113: 167–172.
41. **Isobe N, Terada T.** Effect of the factor inhibiting germinal vesicle breakdown on the disruption of gap junctions and cumulus expansion of pig cumulus-oocyte complexes cultured *in vitro*. *Reproduction* 2001; 121: 249–257.
42. **Phillips DM, Dekel N.** Maturation of the rat cumulus-oocyte complex: structure and function. *Mol Reprod Dev* 1991; 28: 297–306.
43. **Azarnia R, Reddy S, Kmiecik TE, Shalloway D, Loewenstein WR.** The cellular src gene product regulates junctional cell-to-cell communication. *Science* 1988; 239: 398–401.
44. **Crow DS, Beyer EC, Paul DL, Kobe SS, Lau AF.** Phosphorylation of connexin43 gap junction protein in uninfected and Rous sarcoma virus-transformed mammalian fibroblasts. *Mol Cell Biol* 1990; 10: 1754–1763.
45. **Filson AJ, Azarnia R, Beyer EC, Loewenstein WR, Brugge JS.** Tyrosine phosphorylation of a gap junction protein correlates with inhibition of cell-to-cell communication. *Cell Growth Differ* 1990; 1: 661–668.
46. **Kanemitsu MY, Loo LW, Simon S, Lau AF, Eckhart W.** Tyrosine phosphorylation of connexin 43 by v-Src is mediated by SH2 and SH3 domain interactions. *J Biol Chem* 1997; 272: 22824–22831.
47. **Lin R, Warn-Cramer BJ, Kurata WE, Lau AF.** v-Src phosphorylation of connexin 43 on Tyr247 and Tyr265 disrupts gap junctional communication. *J Cell Biol* 2001; 154: 815–827.

CASE REPORT

A birth from the transfer of a single vitrified-warmed blastocyst using intracytoplasmic sperm injection with calcium ionophore oocyte activation in a globozoospermic patient

Koichi Kyono, M.D.,[a] *Yukiko Nakajo, B.S.,*[a] *Chikako Nishinaka, B.S.,*[a] *Hiromitsu Hattori, B.S.,*[a] *Toshihiko Kyoya, B.S.,*[a] *Takayuki Ishikawa, Ph.D.,*[a] *Hiroyuki Abe, Ph.D.,*[b] *and Yasuhisa Araki, Ph.D.*[c]

[a] Kyono ART Clinic, Mitsui-Seimei, Honcho, Aobaku, Sendai; [b] Graduate School of Science and Engineering, Yamagata University, Jyounan, Yonezawa, Yamagata; and [c] Institute for ARMT, Ishii, Fujimi, Setagun, Gunma, Japan

Objective: To present the effectiveness of diagnostic heterologous intracytoplasmic sperm injection (ICSI), mouse oocyte activation test (MOAT), and ICSI combined with assisted oocyte activation (AOA) in a globozoospermic patient.
Design: A case report.
Setting: A private IVF center, Japan.
Patient(s): A patient with globozoospermia.
Intervention(s): MOAT in a mouse and ICSI combined with AOA in a human.
Main Outcome Measure(s): Ultrastructure, MOAT, fertilization, and pregnancy.
Result(s): The transmission electron micrographs showed 100% round-headed spermatozoa lacking an acrosome. MOAT showed that the fertilization rate was 68.4% (13/19) when AOA was used but 0% (0/19) when AOA was not used. After the diagnosis of globozoospermia and sperm-related activation deficiency, 17 human mature oocytes were activated with calcium ionophore after ICSI was performed. The fertilization rate was 88.2% (15/17), and 11 blastocysts were cryopreserved using the vitrification method to prevent severe ovarian hyperstimulation syndrome. A single vitrified-warmed blastocyst was transferred. A gestational sac with fetal heart movements was recognized, and a healthy boy weighing 3180 g was born at 40 weeks of gestation by cesarean section without any congenital abnormality.
Conclusion(s): MOAT allows discrimination between sperm- and oocyte-related fertilization failures and shows the effectiveness of AOA. (Fertil Steril® 2009;91:931.e7–e11. ©2009 by American Society for Reproductive Medicine.)

Key Words: Globozoospermia, calcium ionophore A23187, strontium chloride ($SrCl_2$), ICSI, diagnostic heterologous ICSI, assisted oocyte activation (AOA), round-headed spermatozoa, lack of an acrosome

Globozoospermia is a rare (incidence <0.1% in male infertile patients) form of teratozospermia, mainly characterized by round-headed spermatozoa that lack an acrosome. It originates from a disturbed spermiogenesis, which is known to be genetic. These sperm lack acrosomal membranes and acrosin contents, so they are unable either to penetrate the zona pellucida of an oocyte or to fuse with the oolemma in vivo or in vitro. However, intracytoplasmic sperm injection (ICSI) has opened up new possibilities to couples with male factor infertility caused by globozoospermia (1–9). However, ICSI with globozoospermic cells is generally less successful compared with typical ICSI (10). Rybouchkin et al. (11) discovered that fertilization was improved when a calcium ionophore was used as well. They suggested that the sperm-associated oocyte-activating factor that normally causes the Ca^{2+} flux required for fertilization might be absent or down-regulated in globozoospermic sperm. We report a successful case of pregnancy and delivery from a transfer of a single vitrified-warmed blastocyst after performing ICSI and assisted oocyte activation (AOA) in a patient with globozoospermia and asthenozoospermia.

Received July 29, 2008; revised September 27, 2008; accepted October 3, 2008.
K.K. has nothing to disclose. Y.N. has nothing to disclose. C.N. has nothing to disclose. H.H. has nothing to disclose. T.K. has nothing to disclose. T.I. has nothing to disclose. H.A. has nothing to disclose. Y.A.
Reprint requests: Dr. Koichi Kyono, Kyono ART Clinic, Mitsui-Seimei, Sendai Honcho Bld, 3F, 1-1-1, Honcho, Aobaku, Sendai 980-0014, Japan (FAX: 81-22-722-8840; E-mail: info@ivf-kyono.or.jp).

CASE REPORT

Informed consent was obtained from the couple before the study. The couple, with primary infertility of 2 years' duration, was healthy and had no physical issues except for the

doi:10.1016/j.fertnstert.2008.10.002

FIGURE 1

Round-headed sperm morphology in a globozoospermic patient. **(A)** Normal sperm morphology, control aspects by light microscope. **(B)** Round-headed sperm morphology of a patient by light microscope. **(C)** Round-headed sperm morphology of a patient by electron microscope.

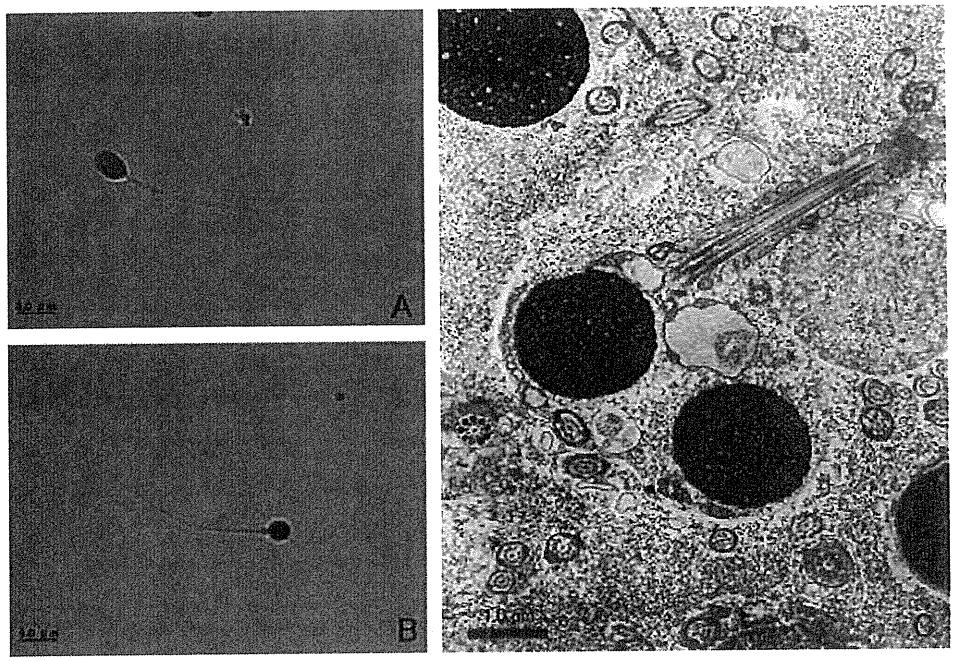

Kyono. Birth from a globozoospermic patient. Fertil Steril 2009.

husband's semen characteristics. A Kruger test showed 100% round-headed sperm with abnormal morphology. We diagnosed the husband as having globozoospermia by electron microscopy. Since we confirmed the efficacy of AOA by mouse oocyte activation test (MOAT), ICSI with AOA was performed for human oocytes.

MATERIALS AND METHODS

Patient History (Anamnesis)

Before this study, we obtained informed consent from the couple and approval from the Institutional Review Board for this study. A 29-year-old woman and her 30-year-old husband presented with primary infertility of 2 years' duration. The couple was healthy and had no physical issues except for the husband's semen aspects. The fertility of the wife was completely normal. Semen analysis showed normal values in volume (2.0 mL), concentration (38×10^6/mL), and motility (39%), which proved asthenozoospermia, and the analysis also showed 100% round-headed sperm with abnormal morphology on light and electron microscopy (Fig. 1). The karyotypes of the couple were 46,XX (wife) and 46,XY (husband) on peripheral lymphocytes.

Fixation and Observation for Electron Microscopy

Sperm were processed for transmission electron microscopy using the method described elsewhere (12), by which they were collected with centrifugation and fixed in chilled 2.5% glutaraldehyde (Wako; Osaka, Japan) solution in 0.1 M phosphate buffer, pH 7.4. After they were washed with chilled 0.1 M phosphate buffer, the sperm were postfixed in chilled 1% osmium teroxide (Taab Laboratories Equipment Ltd., Berkshire, UK) in 0.1 M phosphate buffer, dehydrated in a series of graded ethanol, and embedded in epoxy resin (Taab Laboratories Equipment Ltd.). Ultrathin sections were cut with a diamond knife using an ultramicrotome (Reichert Ultracuts, Leica; Heerbrugg, Switzerland), stained with uranyl acetate and lead citrate, and examined by a transmission electron microscope (IEM-1210, Jeol; Tokyo, Japan).

MOAT

Preparation of mouse oocytes Mature B6D2F1 female mice, 8–12 weeks of age, were superovulated by IP injections of 5 IU pregnant mare serum gonadotropin (PMSG) followed by the administration of 5 IU hCG 48 hours later. The mouse oocytes were collected from the oviducts of the females 14–16 hours after the hCG injection. The oocytes were freed from cumulus cells by pipetting in a Hepes-human follicular fluid medium (Hepes-HFF99; Fuso Pharmaceutical Industries, Osaka, Japan) supplemented with 10% synthetic serum substance (SSS; Irvine Scientific, Santa Ana, CA) and 60 IU/mL bovine testicular hyaluronidase (Sigma Chemical Co., St. Louis) at 37°C. These oocytes were rinsed and kept in an HFF

medium (HFF99; Fuso Pharmaceutical Industries) at 37°C in an atmosphere of 5% CO_2 until the sperm were injected.

Procedures of ICSI and mouse oocyte activation The round-headed sperm of this patient were injected into the mouse oocytes by a piezo-driven unit using the methods reported elsewhere (13–15). The oocyte membranes were broken by applying one or two faint piezo pulses, and the sperm were injected into each ooplasm. It took approximately 20 minutes to inject a group of about 15 oocytes. The injected oocytes were kept for 20–30 minutes at room temperature. During this interval, the oocytes that had been classified into the activation treatment group were activated in a Ca-free Toyoda, Yokoyama, Hoshi (TYH) medium containing 10 mM $SrCl_2$ for 60 minutes at 37°C in an atmosphere of 5% CO_2. These oocytes were transferred one by one into a single 10-μL drop of HFF99 medium with 10% SSS under mineral oil in a plastic dish, and the dish was incubated at 37°C in an atmosphere of 5% CO_2. Approximately 7–11 hours after injections and the activation treatment, the oocytes were observed under an inverted microscope and were rotated to determine whether or not the second polar body and two pronuclei were present.

For the statistical analysis, the obtained data were analyzed by the χ^2-test.

Ovarian Stimulation, Oocyte Collection, and Oocyte Activation in Patient

Ovarian stimulation was conducted using a combination of GnRH agonist (Nasanyl, Yamanouchi, Japan) and hMG (Pergogreen; Serono, Geneva, Swizerland). An injection of 5000 units of hCG (Profasi, Serono) was administered when the dominant follicle reached a mean diameter of 20 mm. Vaginal ultrasound-guided follicle puncture was conducted 36 hours after the hCG injection. The retrieved oocytes were cultured for several hours in Quinn's Advantage Cleavage medium (Sage, Pasadena, CA) at 37°C in an atmosphere of 6% CO_2, 5% O_2, 89% N_2, under humidified conditions, and all oocytes were denuded enzymatically with 70 IU/mL SynVitro Cumulase (MediCult, Copenhagen, Denmark) for 30–60 seconds, followed by mechanical denudation. The motile round-headed sperm were injected into the oocytes in metaphase II, and these oocytes were activated by calcium ionophore A23187 (Sigma;10 μM/mL) for 5 minutes after ICSI. Subsequently, the oocytes were rinsed several times in culture medium and incubated overnight to recognize 2 pronuclei at 37°C in an atmosphere of 6% CO_2, 5% O_2, and 89% N_2 under humidified conditions. For blastocyst cultivation, we transferred the embryos to a sequential medium Quinn Advantage (Sage) or Multi-Blasto Medium (Irvine, CA) on day 3.

Vitrifying and Warming of Blastocysts

All blastocysts were cryopreserved using the vitrification method as described in Kyono et al. (16) to prevent severe ovarian hyperstimulation syndrome (OHSS). The blastocysts were equilibrated for 8–10 minutes in 7.5% ethylene glycol (EG) and 7.5% dimenthyl sulfoxide (DMSO) and then into cryoprotectant 15% EG, 15% DMSO, and 0.5 M sucrose (Kitazato Supply Ltd., Japan) for 1 minute. After that, they were immediately put on a Cryotop and inserted into liquid nitrogen. Warming was performed at room temperature by the rapid thawing method following the market procedure (Kitazato Supply Ltd.). Cryoprotectant was removed by stepwise reduction of the EG and DMSO concentration containing 1.0, 0.5, and 0 M sucrose.

After a single vitrified-warmed blastocyst (grade 5BA) was transferred, a clinical pregnancy was determined by the presence of a gestational sac (GS) and a fetal heartbeat via a transvaginal ultrasound.

RESULTS

The couple did not achieve a pregnancy in spite of repeatedly attempted IUI. We diagnosed the husband as having globozoospermia, which is defined as round-headed sperm lacking an acrosome by the Kruger test and transmission electron microscope (Fig. 1). MOAT was tried but still resulted in no fertilization under piezo-ICSI without activation. As the fertilization rate after $SrCl_2$ activation was increased to 68.4%, it was strongly recommended to pursue the necessary artificial activation to increase the fertilization rate (Table 1).

Round-headed sperm were injected into 17 oocytes during metaphase II. Among the injected oocytes, 15 oocytes were activated (15/17, fertilization rate 88.2%). By day 5, 10 embryos had developed, and another blastocyst developed on the sixth day. Seven of 11 blastocysts were of good morphology, and four blastocysts did not fit the criteria for fair quality. Two months later, one vitrified blastocyst (grade 5BA) was warmed and transferred to the female patient on the fifth day after hormone treatment with P 50 mg (Fuji Pharmaceutical Co., Ltd., Tokyo, Japan). The luteal phase was supported by daily injections of P. After 10 days, pregnancy was established by positive ß-hCG in the serum, and the fetal heartbeat was later confirmed by ultrasound. The couple did not desire amniocentesis so we did not perform it. Fortunately, the female patient remained in good condition throughout the full-term pregnancy. Finally, a healthy boy weighing 3180 g was delivered at 40 weeks of gestation by cesarean section.

DISCUSSION

ICSI is a useful technique for men who are infertile because of round-headed sperm. ICSI has led to fertilization, embryo development, pregnancy, and delivery of infants (1–9). However, several investigators have reported low to absent fertilization (2, 4, 5, 17, 18). Rybouchkin et al. (11) discovered that fertilization was improved when a calcium ionophore was added. They suggested that a sperm-associated oocyte-activating factor that normally causes the Ca^{2+} flux required for fertilization might be absent or down-regulated in globozoospermic sperm, a suggestion that was subsequently confirmed by several studies (11, 19, 20). Subsequently, Rybouchkin et al. in 1997 (18), Kim et al. in 2001 (21),

TABLE 1

Results of injected round-headed sperm to mouse oocytes and activation.

	Activation (+)	Activation (−)
No. of oocytes with ICSI	22	20
No. of surviving oocytes	21	19
Normal morphology	19	19
Abnormal morphology	0	0
2PN 2PB (+)	13 (68.4)	0
2PN 2PB (−)	1 (5.3)	0
1PN 2PB (+)	3 (15.8)	0
3PN 2PB (−)	2 (10.5)	0
0PN 2PB (+)	0	0
0PN 2PB (−)	0	19 (100)
Total activated oocytes	19 (100)	0 (0)

Note: Data in parentheses are percents. Activation (+): The activation treatment group was activated in a Ca-free TYH medium containing 10 mM $SrCl_2$ for 60 minutes at 37°C in an atmosphere of 5% CO_2. The details are mentioned in Materials and Methods. 2PN = two pronuclei formation; 2PB = first and second polar body.

Kyono. Birth from a globozoospermic patient. Fertil Steril 2009.

Heindryckx et al. in 2005 (15), and Tajera et al. in 2008 (22) reported successful pregnancies and deliveries using ICSI with calcium ionphore oocyte activation. On the other hand, Tesarik et al. in 2002 (14) reported that the possibility of using a simple modification of the standard ICSI micromanipulation technique, instead of ionophores, alleviates concerns about the possible harmful effects to human embryos of these insufficiently tested drugs. Vigorous aspiration of oocyte cytoplasm and repeated in-and-out movements of the microinjection needle within the human oocyte during the ICSI produce a considerable influx of calcium ions from the surrounding culture medium into the oocyte. It is also possible that mechanical disruption of endoplasmic reticulum during the movements of the microinjection needle in the oocyte cytoplasm and repeated aspiration releases the calcium stored in this organelle. The modified ICSI technique increases the intracellular concentrations of the free calcium ion in the injected oocyte compared with the standard ICSI technique.

Electrical stimulation, ethanol, $SrCl_2$, Ca ionophore, and vigorous ICSI have been reported as AOA. Ca ionophore, ethanol 8%, and $SrCl_2$ (from our data) displayed the efficacy of AOA for globozoospermia in heterologous ICSI models. Ca ionophore and vigorous ICSI were reported to have the effectiveness of AOA for globozoospermia in human ICSI clinically, but electrical stimulation, ethanol, and $SrCl_2$ are not yet reported to be effective. More studies are needed to examine which method is truly the best for AOA in globozoospermia.

This couple had tried IUI three times; however, they did not achieve pregnancy. First, we diagnosed the husband as having globozoospermia. Second, we compared the results with and without oocyte activation using $SrCl_2$ on mouse oocytes with round-headed sperm injection. From the outcomes of MOAT, we concluded that round-headed sperm might lack the ability of oocyte activation. We reported the efficacy and the safety of $SrCl_2$ in the patients with low fertilization by ICSI (23). However, the $SrCl_2$ activator is not yet approved for use with human oocytes in the case of globozoospermia. Third, in this case, we tried calcium ionophore A23187 treatment, which was also reported by several investigators (18, 19, 22, 23) to activate human oocytes injected with round-headed sperm. The fertilization rate in our case is 82.2% (15 of 17), which may be attributed to the AOA with calcium ionophore A23187 treatment. We believe that oocyte activation after ICSI using round-headed sperm is vital.

Edirisinghe et al. (24) studied the cytogenetics of unfertilized oocytes after ICSI. Failure of activation and the consequent failure of the oocyte to complete meiosis II were likely to have contributed to the high rate of premature chromatin condensation seen in their cases. These data suggest that round-headed sperm lack the capacity to penetrate oocytes and may also be deficient in their oocyte-activating ability.

Generally, round-headed sperm were observed to have a comparatively higher chance of abnormal aneuploidy chromosome (25–27), and chromatin structure and centrosomal function had activated abnormally in globozoospermia (28–30).

Although karyotypes of round-headed sperm have not been discussed in many nuclear studies in great detail, several articles have reported on aneuploidy, centrosomal dysfunction, and chromatid structure abnormalities. More studies regarding the karyotypes of rounded-headed sperm are necessary in the future. Round-headed sperm are deficient in oocyte-activation capacity, and this deficiency is independent of the variation in morphology of the sperm heads. The most probable reason for this deficiency is the absence or down-regulation of the sperm oocyte-activating factor in these sperm. Further investigation of globozoospermia would give valuable information on the general mechanism of spermatogenesis; different aspects of sperm-egg interaction; and physiology, etiology, and chromosome aneuploidy of globozoospermia.

In summary, we report a successful pregnancy and delivery from a transfer of a single vitrified-warmed blastocyst after performing ICSI with round-headed sperm and AOA in a globozoospermic patient.

REFERENCES

1. Lundin K, Sjogren A, Nilsson L, Hamberger L. Fertilization and pregnancy after intracytoplasmic microinjection of acrosomeless spermatozoa. Fertil Steril 1994;62:1266–7.
2. Liu J, Nagy Z, Joris H, Tournaye H, Devroey P, Van Steirteghem A. Successful fertilization and establishment of pregnancies after intracytoplasmic sperm injection in patients with globozoospermia. Hum Reprod 1995;10:626–9.
3. Trokoudes KM, Danos N, Kalogirou L, Vlachou R, Lysiotis T, Georghiades N, et al. Pregnancy with spermatozoa from a globozoospermic man after intracytoplasmic sperm injection treatment. Hum Reprod 1995;10:880–2.
4. Kilani ZM, Shaban MA, Ghunaim SD, Keilani SS, Dakkak AI. Triplet pregnancy and delivery after intracytoplasmic injection of round-headed spermatozoa. Hum Reprod 1998;13:2177–9.
5. Stone S, O'Mahony F, Khalaf Y, Taylor A, Braude P. A normal live birth after intracytoplasmic sperm injection for globozoospermia without assisted oocyte activation. Hum Reprod 2000;15:139–41.
6. Coetzee K, Windt ML, Menkveld R, Kruger TF, Kitshoff M. An intracytoplasmic sperm injection pregnancy with a globozoospermic male. J Assist Reprod Genet 2001;18:311–3.
7. Nardo LG, Sinatra F, Bartoloni G, Zafarana S, Nardo F. Ultrastructural features and ICSI treatment of severe teratozoospermia: report of two human cases of globozoospermia. Eur J Obstet Gynecol Reprod Biol 2002;104:40–2.
8. Zeyneloglu HB, Baltaci V, Duran HE, Erdemli E, Batioglu S. Achievement of pregnancy in globozoospermia with Y chromosome microdeletion after ICSI. Hum Reprod 2002;17:1833–6.
9. Kilani Z, Ismail R, Ghunaim S, Mohamed H, Hughes D, Brewise I, et al. Evaluation and treatment of familial globozoospermia in five brothers. Fertil Steril 2004;82:1436–9.
10. Dam AH, Frenstra I, Westphal JR, Ramos L, Van Golde RJ, Kremer JA. Globozoospermia revisited. Hum Reprod Update 2007;13:63–75.
11. Rybouchkin AV, Dozortsev D, Pelinck MJ, De Sutter P, Dhont M. Analysis of the oocyte activating capacity and chromosomal complement of round-headed human spermatozoa by their injection into mouse oocytes. Hum Reprod 1996;11:2170–5.
12. Abe H, Otoi T, Tachikawa S, Yamashita S, Satoh T, Hopshi H. Fine structure of bovine morulae and blastocysts in vivo and in vitro. Anat Embryol 1999;199:519–27.
13. Araki Y, Yoshizawa M, Abe H, Murase Y, Araki Y. Use of mouse oocytes to evaluate the ability of human sperm to activate oocytes after failure of activation by intracytoplasmic sperm injection. Zygote 2004;12:111–6.
14. Tesarik J, Rienzi L, Ubaldi F, Mendoza C, Greco E. Use of a modified intracytoplasmic sperm injection technique to overcome sperm-borne and oocyte-borne oocyte activation failures. Fertil Steril 2002;78:619–24.
15. Heindryckx B, Van del Elst J, De Sutter P, Dhont M. Treatment option for sperm- or oocyte-related fertilization failure: assisted oocyte activation following diagnostic heterologous ICSI. Hum Reprod 2005;20:2237–41.
16. Kyono K, Nakajo Y, Kumagai S, Nishinaka C. Vitrifying and warming of oocytes using cryotop. In: Tucker MJ, Liebermann J, eds. Vitrification in Assisted Reproduction. A User's Manual and Trouble-Shooting Guide: Informa UK Ltd., 2007:153–61.
17. Battaglia DE, Koehler JK, Klein NA, Tucker MJ. Failure of oocyte activation after intracytoplasmic sperm injection using round-headed sperm. Fertil Steril 1997;68:118–22.
18. Rybouchkin AV, Van der Straeten F, Quatacker J, De Sutter P, Dhont M. Fertilization and pregnancy after assisted oocyte activation and intracytoplasmic sperm injection in a case of round-headed sperm associated with deficient oocyte activation capacity. Fertil Steril 1997;68:1144–7.
19. Gomez E, Perez-Cano I, Amorocho B, Landeras J, Ballesteros A, Pellicer A. Effect of injected spermatozoa morphology on the outcome of intracytoplasmic sperm injection in humans. Fertil Steril 2000;74:842–3.
20. Schmiady H, Schulze W, Scheiber I, Pfuller B. High rate of premature chromosome condensation in human oocytes following microinjection with round-headed sperm: case report. Hum Reprod 2005;20:1319–23.
21. Kim ST, Cha YB, Park JM, Gye MC. Successful pregnancy and delivery from frozen-thawed embryos after intracytoplasmic sperm injection using round-headed spermatozoa and assisted oocyte activation in a globozoospermic patient with mosaic Down syndrome. Fertil Steril 2001;75:445–7.
22. Tajera A, Molla M, Muriel L, Remohi J, Pellicer A, De Pablo JL. Successful pregnancy and childbirth after intracytoplasmic sperm injection with calcium ionophore oocyte activation in a globozoospermic patient. Fertil Steril 2008;90:1202.e1–e5.
23. Kyono K, Kumagai S, Nishinak C, Nakajo Y, Uto H, Toya M, et al. Birth and follow-up of babies born following ICSI using SrCl2 oocyte activation. RBM Online 2008;17:53–8.
24. Edirisinghe WR, Murch AR, Junk SM, Yovich JL. Cytogenetic analysis of unfertilized oocytes following intracytoplasmic sperm injection using spermatozoa from a globozoospermic man. Hum Reprod 1998;13:3094–8.
25. Martin RH, Greene C, Rademaker AW. Sperm chromosome aneuploidy analysis in a man with globozoospermia. Fertil Steril 2003;79(Suppl 3):1662–4.
26. Morel F, Douet-Guilbert N, Moerman A, Duban B, Marchetti C, Delobel B, et al. Chromosome aneuploidy in the spermatozoa of two men with globozoospermia. Mol Hum Reprod 2004;10:835–8.
27. Ditzel N, El-Danasouri I, Just W, Sterzik K. Higher aneuploidy rates of chromosomes 13, 16, and 21 in a patient with globozoospermia. Fertil Steril 2005;84:217–8.
28. Vicari E, Perdichizzi A, De Palma A, Burrello N, D'Agata R, Calogero AE. Globozoospermia is associated with chromatin structure abnormalities: case report. Hum Report 2002;17:2128–33.
29. Larson KL, Brannian JD, Singh NP, Burbach JA, Jost LK, Hansen KP, et al. Chromatin structure in globozoospermia: a case report. J Androl 2001;22:424–31.
30. Nakamura S, Terada Y, Horiuchi T, Emuta C, Murakami T, Yaegashi N, et al. Analysis of the human sperm centrosomal function and the oocyte activation ability in a case of globozoospermia, by ICSI into bovine oocytes. Hum Reprod 2002;17:2930–4.